



## Closed-loop identification of unstable systems using noncausal FIR models

Khaled F. Aljanaideh & Dennis S. Bernstein

To cite this article: Khaled F. Aljanaideh & Dennis S. Bernstein (2017) Closed-loop identification of unstable systems using noncausal FIR models, International Journal of Control, 90:2, 184-201, DOI: [10.1080/00207179.2016.1172733](https://doi.org/10.1080/00207179.2016.1172733)

To link to this article: <http://dx.doi.org/10.1080/00207179.2016.1172733>



Accepted author version posted online: 08 Apr 2016.  
Published online: 28 Apr 2016.



Submit your article to this journal [↗](#)



Article views: 107



View related articles [↗](#)



View Crossmark data [↗](#)

## Closed-loop identification of unstable systems using noncausal FIR models

Khaled F. Aljanaideh and Dennis S. Bernstein

Department of Aerospace Engineering, The University of Michigan, Ann Arbor, MI, USA

### ABSTRACT

Noncausal finite impulse response (FIR) models are used for closed-loop identification of unstable multi-input, multi-output plants. These models are shown to approximate the Laurent series inside the annulus between the asymptotically stable pole of the largest modulus and the unstable pole of the smallest modulus. By delaying the measured output relative to the measured input, the identified FIR model is a noncausal approximation of the unstable plant. We present examples to compare the accuracy of the identified model obtained using least squares, instrumental variables methods, and prediction error methods for both infinite impulse response (IIR) and noncausal FIR models under arbitrary noise that is fed back into the loop. Finally, we reconstruct an IIR model of the system from its stable and unstable parts using the eigensystem realisation algorithm.

### ARTICLE HISTORY

Received 8 June 2015  
Accepted 28 March 2016

### KEYWORDS

Closed-loop identification;  
noncausal FIR models

### 1. Introduction

Identification of a plant operating inside a closed loop is motivated by the need to monitor plant changes without opening the loop (Gustavsson, Ljung, & Söderström, 1977; Hjalmarsson, Gevers, & de Bruyne, 1996; Landau, 2001). This need is unavoidable when the controlled plant is open-loop unstable, in which case opening the loop for identification is prohibited. Even for plants that are asymptotically stable, opening the loop for identification may not be feasible due to operational constraints. In these cases, identification must rely on sensor–actuator data obtained under normal operating conditions, although in some cases it may be possible to inject additional signals to enhance persistency and signal amplitude relative to noise levels.

In addition to the fact that closed-loop identification constrains the feasible inputs, output noise and process noise inside the feedback loop are correlated with the control input. Although knowledge of this correlation may enhance the accuracy of system identification, this information is usually not available in practice, and decorrelation techniques are needed (Söderström & Stoica, 2002, 1981; Stoica, Söderström, & Friedlander, 1985). In Ljung (2002) and Forssell and Ljung (1999), an infinite impulse response (IIR) model is used with prediction error methods (PEM) to identify unstable systems in closed loop. Assuming that the output noise and process noise are uncorrelated with the command signal, applying PEM with either the true system order or an overestimated system order guarantees that the estimated transfer function

converges to the true transfer function as the number of samples used for identification tends to infinity (Ljung, 2002). However, for a finite data set, overestimating the system order can yield poor transfer function estimates.

If the plant order is unknown, then an initial overestimate of the order can be used with PEM, and a refined estimate can be obtained from Ho–Kalman realisation theory (Ho & Kalman, 1966) and its implementation in terms of the singular value decomposition of the Hankel matrix (Juang, 1993). Although this approach, which requires estimates of the Markov (impulse response) parameters, is sensitive to noise, heuristics can be used to improve its accuracy (Hjalmarsson, Welsh, & Rojas, 2012; Markovsky, 2012; Recht, Fazel, & Parrilo, 2010; Smith, 2014; Usevich & Markovsky, 2012).

PEM identification minimises the difference between the predicted output and the measured output, which yields an estimate of the transfer function. If the predictor is unstable, which is the case when output-error and Box–Jenkins model structures are used to identify unstable systems in closed loop (Forssell & Ljung, 2000b), the prediction error may be large, which leads to erroneous transfer function estimates. This issue can be mitigated by using modified output-error and Box–Jenkins models as in Forssell and Ljung (2000b), where the predictor is constrained to be stable. However, this constraint complicates the search algorithm (Forssell & Ljung, 2000b).

An alternative approach to PEM identification of unstable plants is discussed in Hjalmarsson and Forssell (1999), where an output-error model structure is considered. In this case, the predictor is decomposed into stable

and unstable parts, which correspond to causal and non-causal filters, respectively. A model is noncausal if computing the output at time  $k$  requires inputs at a future time  $k + i$ , where  $i \geq 1$ . Since output-error models are a special type of IIR models, this approach requires an estimate of the order of the system. However, as discussed above, if the estimated order is incorrect, then the transfer function estimates may have poor accuracy. In addition, identifying the noncausal part of the model requires time-reversing the signal and thus is confined to offline identification. Moreover, the approaches used in Hjalmarsson and Forsell (1999) and Forsell and Ljung (2000b) require a priori knowledge of whether the system is stable or unstable.

Noncausal filtering is also used in Forsell and Ljung (2000a) in a two-step projection method to identify systems in closed loop with nonlinear feedback. A noncausal finite impulse response (FIR) model is first used with linear least mean squares optimisation to identify the causal closed-loop system from the command signal to the control input. Then, the identified model is used with the command signal to compute the predicted control input, which is then compared with the output of the closed-loop system to identify the plant using an IIR model. The role of the noncausal FIR model in Forsell and Ljung (2000a) is restricted to approximating the Wiener smoother, which relates the command signal to the control input.

Instrumental variables can also be used to identify unstable systems in closed loop, where the instruments consist of samples of either the command signal or a pre-filtered version of the command signal (Gilson & Van den Hof, 2005; Söderström & Stoica, 2002). Subspace methods can also be used to identify linear systems in closed loop (Ljung & McKelvey, 1996; Verhaegen, 1993).

The usefulness of Markov parameters for estimating the order of an IIR system suggests consideration of an FIR model structure, whose numerator coefficients are its Markov parameters and all of whose poles are zero. Although physical systems are rarely FIR, an FIR model can approximate an asymptotically stable, IIR system (Cerone, Piga, & Regruto, 2013; Chai, Zhang, Zhang, & Mosca, 2005; Yamamoto, Anderson, Nagahara, & Koyanagi, 2003). An advantage of FIR models for system identification is that the Markov parameters of an FIR model are given explicitly, and thus can be used directly in Ho–Kalman realisation to estimate the system order and construct an IIR model. Most importantly, the FIR model structure is nonparametric in the sense that it is independent of the system poles and zeros, and thus no prior estimate of the plant order is needed.

Noncausal FIR controllers are used for tracking problems where the command signal is known in advance.

In particular, a noncausal FIR feedforward controller is obtained by truncating the Laurent series of the unstable inverse of a nonminimum-phase plant; the resulting controller provides approximate plant inversion without unstable pole-zero cancellation (Gross, Tomizuka, & Messner, 1994; Hunt, Meyer, & Su, 1996; Rigney, Pao, & Lawrence, 2009; Tomizuka, 1987; Widrow & Walach, 1996).

A noncausal FIR model that approximates the Laurent series of an unstable plant involves both positive and negative powers of the Z-transform variable  $z$ . The negative powers approximate the asymptotically stable part of the plant outside of a disk (that is, inside a punctured plane), whereas the positive powers approximate the unstable part of the plant inside a disk. Inside the common region, which is an annulus, the Laurent series represents a noncausal model, as evidenced by the positive powers of  $z$ .

To identify an unstable plant operating inside a stabilising feedback loop, the measured output can be delayed relative to the measured input to obtain an FIR model that is a noncausal approximation of the unstable plant. The transfer function of this noncausal FIR model approximates the Laurent series of the plant inside the maximal annulus of analyticity lying between the smallest disk containing the asymptotically stable poles and the smallest punctured plane containing the unstable poles.

Although advantages of noncausal filters were observed in Hjalmarsson and Forsell (1999) and Forsell and Ljung (1999), a full justification is lacking. One of the contributions of the present paper is thus to use the Laurent expansion of a rational transfer function to justify the use of these models in system identification. The contribution of the present paper is thus a detailed treatment of closed-loop identification of unstable plants using noncausal FIR models. This work presents analysis and proofs that connect the Laurent series of a transfer function and an associated noncausal FIR model. These results are needed to establish a rigorous connection between the estimated noncausal FIR model and the impulse response of the system. Unlike the noncausal output-error models identified in Hjalmarsson and Forsell (1999), noncausal FIR models can be identified online. Moreover, unlike the approaches of Hjalmarsson and Forsell (1999) and Forsell and Ljung (2000b), noncausal FIR models do not require knowledge of whether the system is stable or unstable.

The theoretical basis for this work is given by [Theorem 4.1](#), which provides necessary and sufficient conditions under which the coefficients of the Laurent series are square summable. In addition, [Theorem 4.1](#) shows that there is exactly one maximal annulus corresponding to which the coefficients of the Laurent series are bounded. This fact suggests that the objective of identifying  $G$  by

estimating the coefficients of a Laurent series of  $G$  is meaningful only for the Laurent series corresponding to this special annulus, since otherwise the unidentified (that is, truncated) coefficients are unbounded. For unstable plants, the Markov parameters, which are the coefficients of the Laurent series in the maximal punctured plane, are unbounded. For unstable plants, however, the Laurent series in the special annulus has (unlike the Laurent series in the punctured plane) terms involving positive powers of  $z$ , which represent a non-causal model. The coefficients of the negative powers of  $z$  are Markov parameters of the asymptotically stable part of the transfer function.

These results refine and extend (Aljanaideh, Coffey, & Bernstein, 2013) to the case of MIMO systems. Furthermore, unlike identification based on least squares in Aljanaideh et al. (2013), the present paper applies prediction error methods and instrumental variables methods to closed-loop identification of unstable systems with IIR and noncausal FIR models. Finally, we extend (Aljanaideh et al., 2013) by demonstrating consistency of the estimated FIR coefficients under noise added to the input and output signals of the plant inside the loop.

The analysis in this paper is carried out within the context of idealised finite-dimensional rational transfer functions, where the goal is to assess the accuracy of identification of unstable plants operating inside a closed loop using noncausal FIR models. In practice, however, realistic plants do not conform to mathematical models, and concepts such as system order, transfer function, and the like are convenient but fictitious constructions used to approximate reality. Moreover, for the purpose of controller design, an appropriate notion of model order may be different from the ‘true’ order, and may hinge on the dominant modes of the system as well as uncertainty of the identified model. These issues are, however, outside the scope of this paper.

The contents of the paper are as follows. In Section 2, we present definitions and results needed for the rest of the paper. Section 3 provides analysis of the Laurent series of a rational function. Section 4 shows the necessary and sufficient conditions for boundedness of the Laurent series coefficients. Section 5 shows the identification architecture using least squares, instrumental variables, and prediction error methods. We show numerical examples in Section 6. Section 7 discusses how to reconstruct the system from its noncausal FIR model. We give conclusions and suggestions for future research in Section 8.

## 2. Preliminaries

For  $\rho > 0$ , let  $\mathbb{D}(\rho) \triangleq \{z \in \mathbb{C} : |z| < \rho\}$  be the open disk in the complex plane centred at the origin with radius  $\rho$ .

Also, for  $\rho \geq 0$ , let  $\mathbb{P}(\rho) \triangleq \{z \in \mathbb{C} : |z| > \rho\}$  be the open punctured plane centred at the origin with inner radius  $\rho$ . Moreover, for  $0 \leq \rho_1 < \rho_2$ , let  $\mathbb{A}(\rho_1, \rho_2) \triangleq \{z \in \mathbb{C} : \rho_1 < |z| < \rho_2\} = \mathbb{P}(\rho_1) \cap \mathbb{D}(\rho_2)$  be the open annulus in the complex plane centred at the origin with inner radius  $\rho_1$  and outer radius  $\rho_2$ .

Recall (Gamelin, 2001, p. 168) that if the rational function  $g(z)$  is analytic in the open annulus  $\mathbb{A}(\rho_1, \rho_2)$ , then  $g(z)$  has a unique, absolutely convergent Laurent series in  $\mathbb{A}(\rho_1, \rho_2)$  of the form

$$g(z) = \sum_{i=-\infty}^{\infty} h_i z^i. \quad (1)$$

If  $\rho_2 = \infty$ , then  $g$  is analytic in the punctured plane  $\mathbb{P}(\rho_1)$  and, if  $g$  is proper, then, for all  $i > 0$ ,  $h_i = 0$  in (1). If  $\rho_1 = 0$  and  $g$  has no pole at zero, then  $g$  is analytic in the disk  $\mathbb{D}(\rho_2)$  and, for all  $i < 0$ ,  $h_i = 0$  in (1). In this case, (1) is a power series that converges absolutely in  $\mathbb{D}(\rho_2)$  and diverges at every point in  $\mathbb{P}(\rho_2)$  (Gamelin, 2001, p. 138).

**Definition 2.1:** Let  $0 \leq \rho_1 < \rho_2$  and let  $g$  be a rational function. If  $\rho_1 > 0$ , then the open annulus  $\mathbb{A}(\rho_1, \rho_2)$  is *maximal* with respect to  $g$  if  $g$  is analytic in  $\mathbb{A}(\rho_1, \rho_2)$  and, for all  $\epsilon_1 \in [0, \rho_1)$  and  $\epsilon_2 \geq 0$ , not both zero,  $g$  is not analytic in  $\mathbb{A}(\rho_1 - \epsilon_1, \rho_2 + \epsilon_2)$ . If  $\rho_1 = 0$ , then the open disk  $\mathbb{D}(\rho_2)$  is maximal with respect to  $g$  if  $g$  is analytic in  $\mathbb{D}(\rho_2)$  and, for all  $\epsilon > 0$ ,  $g$  is not analytic in  $\mathbb{D}(\rho_2 + \epsilon)$ .

For convenience, the term maximal open annulus may also refer to an open disk or an open punctured plane.

Consider the system

$$x(k+1) = Ax(k) + Bu(k), \quad (2)$$

$$y(k) = Cx(k) + Du(k), \quad (3)$$

where  $A \in \mathbb{R}^{n \times n}$ ,  $B \in \mathbb{R}^{n \times m}$ ,  $C \in \mathbb{R}^{l \times n}$ ,  $D \in \mathbb{R}^{l \times m}$ . Assume that  $(A, B)$  is controllable and  $(A, C)$  is observable. Let  $G$  be the  $l \times m$  transfer matrix corresponding to  $(A, B, C, D)$ . The  $i$ th Markov parameter  $H_i$  of  $G$ , which is given by

$$H_i \triangleq \begin{cases} D, & i = 0, \\ CA^{i-1}B, & i \geq 1, \end{cases} \quad (4)$$

is independent of the realisation (2), (3) of  $G$ . Let  $\rho(A)$  denote the spectral radius of  $A$ .

**Proposition 2.1:**  $\{H_i\}_{i=0}^{\infty}$  are the coefficients of the Laurent series of  $G$  in  $\mathbb{P}(\rho(A))$ , that is, for all  $z \in \mathbb{P}(\rho(A))$ ,

$$G(z) = \sum_{i=0}^{\infty} H_i z^{-i}. \quad (5)$$

Next, we define the reflected transfer matrix  $G_{\text{ref}}$  to be the transfer matrix obtained by replacing  $z$  in  $G(z)$  by  $z^{-1}$ , that is,  $G_{\text{ref}}(z) = G(z^{-1})$ .

**Proposition 2.2:** Assume that  $A$  is nonsingular. Then,  $G_{\text{ref}}$  is proper, and  $(A^{-1}, -A^{-1}B, CA^{-1}, D - CA^{-1}B)$  is a minimal realisation of  $G_{\text{ref}}$ .

**Definition 2.2:** The spectral radius  $\rho(G)$  of  $G$  is the spectral radius of  $A$ .

**Definition 2.3:** Assume that  $A$  is nonsingular. Then, the inner spectral radius  $\rho_{\text{inner}}(A)$  of  $A$  is defined as

$$\rho_{\text{inner}}(A) \triangleq \frac{1}{\rho(A^{-1})}.$$

Furthermore, the inner spectral radius  $\rho_{\text{inner}}(G)$  of  $G$  is the inner spectral radius of  $A$ .

**Proposition 2.3:** Assume that zero is not a pole of  $G$ . Then,

$$\rho_{\text{inner}}(G_{\text{ref}}) = \frac{1}{\rho(G)}, \quad \rho(G_{\text{ref}}) = \frac{1}{\rho_{\text{inner}}(G)}. \quad (6)$$

**Definition 2.4:**  $G$  is strongly unstable if it has no poles in the closed unit disk.

**Proposition 2.4:**  $G$  is strongly unstable if and only if  $G_{\text{ref}}$  is asymptotically stable.

### 3. Analysis of the Laurent series

Throughout this section, let  $G$  be a proper  $l \times m$  rational function with minimal realisation  $(A, B, C, D)$ . If  $A$  is nonsingular, then the Markov parameters of  $G_{\text{ref}}$  are given by

$$\tilde{H}_i \triangleq \begin{cases} D - CA^{-1}B, & i = 0, \\ -CA^{-i-1}B, & i \geq 1. \end{cases} \quad (7)$$

Therefore, if  $A$  is nonsingular, then Propositions 2.1 and 2.3 imply that the Laurent series of  $G_{\text{ref}}$  in  $\mathbb{P}(\rho(G_{\text{ref}})) = \mathbb{P}(\rho(A^{-1})) = \mathbb{P}(1/\rho(A))$  is given by

$$G_{\text{ref}}(z) = \sum_{i=0}^{\infty} \tilde{H}_i z^{-i}. \quad (8)$$

The following result shows that (7) provides the coefficients of the power series for  $G$  in the maximal disk.

**Proposition 3.1:** Assume that zero is not a pole of  $G$ . Then, for all  $z \in \mathbb{D}(\rho_{\text{inner}}(G))$ ,

$$G(z) = \sum_{i=0}^{\infty} \tilde{H}_i z^i, \quad (9)$$

where  $\tilde{H}_i$  are the Markov parameters of  $G_{\text{ref}}$  given by (7).

**Proof:** Replacing  $z \in \mathbb{P}(\rho(G_{\text{ref}})) = \mathbb{P}(1/\rho_{\text{inner}}(G))$  in (8) by  $z^{-1} \in \mathbb{D}(\rho_{\text{inner}}(G))$  and using the fact that, for all  $z \in \mathbb{P}(\rho(G_{\text{ref}}))$ ,  $G_{\text{ref}}(1/z) = G(z)$  yields (9). ■

Using partial fractions,  $G$  can be represented as

$$G = G_s + G_u + D, \quad (10)$$

where the strictly proper transfer functions  $G_s$  and  $G_u$  are asymptotically stable and strongly unstable, respectively. Defining  $\rho_s \triangleq \rho(G_s)$ , Proposition 2.1 implies that  $G_s$  is analytic in  $\mathbb{P}(\rho_s)$  with the Laurent series

$$G_s(z) = \sum_{i=1}^{\infty} H_{s_i} z^{-i}, \quad (11)$$

where, for all  $i \geq 0$ ,  $H_{s_i}$  is the  $i$ th Markov parameter of  $G_s$ . Next, note that zero is not a pole of  $G_u$ . Hence, defining  $\rho_u \triangleq \rho_{\text{inner}}(G_u)$ ,  $G_u$  is analytic in  $\mathbb{D}(\rho_u)$  with the power series

$$G_u(z) = \sum_{i=0}^{\infty} H_{u_i} z^i, \quad (12)$$

where, by Proposition 3.1,  $H_{u_i}$  is the  $i$ th Markov parameter of  $G_{u, \text{ref}}$ . Rewriting (12) as

$$G_u(z) = \sum_{i=-\infty}^0 H_{u_i} z^{-i}, \quad (13)$$

it follows from (10), (11), and (13) that  $G$  is analytic in the annulus  $\mathbb{A}(\rho_s, \rho_u)$  with the Laurent series

$$G(z) = \sum_{i=-\infty}^{\infty} L_i z^{-i}, \quad (14)$$

where

$$L_i \triangleq \begin{cases} H_{u_i}, & i < 0, \\ H_{u_0} + D, & i = 0, \\ H_{s_i}, & i > 0. \end{cases} \quad (15)$$

Note that the Laurent series of  $G$  in  $\mathbb{A}(\rho_s, \rho_u)$  given by (14) is different from the Laurent series of  $G$  in  $\mathbb{P}(\rho(G))$  given by (5). Furthermore, both  $D = G(\infty)$  and  $H_{u_0} = G_{u, \text{ref}}(\infty)$  may be nonzero.

Assume that  $G$  has no poles on the unit circle. Let  $d$  and  $r$  be positive integers, and define the FIR truncations  $G_{s, r}$  and  $G_{u, d}$  of  $G_s(z)$  and  $G_u(z^{-1})$ , respectively, by

$$G_{s, r}(z) \triangleq \sum_{i=1}^r H_{s_i} z^{-i}, \quad G_{u, d}(z^{-1}) \triangleq \sum_{i=0}^d H_{u_i} z^{-i}, \quad (16)$$

where  $H_{s_i}$  and  $H_{u_{-i}}$  are defined by (15). Note that

$$G_{s,r}(z) = \sum_{i=1}^r L_i z^{-i}, \quad G_{u,d}(z) = \sum_{i=0}^d L_{-i} z^i = \sum_{i=-d}^0 L_i z^{-i}. \tag{17}$$

Now, define the improper rational function  $G_{r,d}(z)$  by

$$G_{r,d} \triangleq G_{s,r} + G_{u,d} + D, \tag{18}$$

where  $G_{s,r}(z)$  and  $G_{u,d}(z)$  are the causal and noncausal components of  $G_{r,d}$ , respectively. Hence, for all  $z \neq 0$ ,

$$G_{r,d}(z) = \sum_{i=-d}^r L_i z^{-i}. \tag{19}$$

#### 4. Necessary and sufficient conditions for boundedness of the Laurent series coefficients

Throughout this section, let  $G$  be an  $l \times m$  proper rational function. Let  $\|\cdot\|_F$  denote the Frobenius norm.

For asymptotically stable and strongly unstable transfer functions, the following result, which is used in the proof of Theorem 4.1, concerns boundedness of the coefficients of the Laurent series of a rational function.

**Lemma 4.1:** *The following statements hold:*

- (i) *Assume that zero is not a pole of  $G$ . If the coefficients (7) of the power series (9) of  $G$  in  $\mathbb{D}(\rho_{\text{inner}}(G))$  are bounded, then  $\rho_{\text{inner}}(G) \geq 1$ .*
- (ii) *If the coefficients (4) of the Laurent series (5) of  $G$  in  $\mathbb{P}(\rho(G))$  are bounded, then  $\rho(G) \leq 1$ .*

**Proof:**

- (i) It follows from Gamelin (2001, p. 142) that the radius of convergence of the power series (9) of  $G$  in  $\mathbb{D}(\rho_{\text{inner}}(G))$  is given by  $\rho_{\text{inner}} = \frac{1}{\limsup_{i \rightarrow \infty} |\tilde{H}_i|^{1/i}}$ .

Define the positive number  $M \triangleq \sup_i |\tilde{H}_i|$ . Then,

$$\rho_{\text{inner}}(G) = \frac{1}{\limsup_{i \rightarrow \infty} |\tilde{H}_i|^{1/i}} \geq \frac{1}{\lim_{i \rightarrow \infty} M^{1/i}} = 1.$$

- (ii) Assume that zero is not a pole of  $G_{\text{ref}}$ . Proposition 3.1 implies that the power series of  $G_{\text{ref}}$  in  $\mathbb{D}(\rho_{\text{inner}}(G_{\text{ref}}))$  is given by (9), where the coefficients of the power series of  $G_{\text{ref}}$  in  $\mathbb{D}(\rho_{\text{inner}}(G_{\text{ref}}))$  are the Markov parameters of  $(G_{\text{ref}})_{\text{ref}} = G$ , which are given by (4). It follows from Gamelin (2001, p. 142) that the radius of convergence of the power series of  $G_{\text{ref}}$  in  $\mathbb{D}(\rho_{\text{inner}}(G_{\text{ref}}))$  is given by  $\rho_{\text{inner}} = \frac{1}{\limsup_{i \rightarrow \infty} |H_i|^{1/i}}$ . Define the positive number  $M \triangleq$

$\sup_i |H_i|$ . Then,

$$\begin{aligned} \frac{1}{\rho(G)} &= \rho_{\text{inner}}(G_{\text{ref}}) = \frac{1}{\limsup_{i \rightarrow \infty} |H_i|^{1/i}} \\ &\geq \frac{1}{\lim_{i \rightarrow \infty} M^{1/i}} = 1. \end{aligned}$$

Now assume that  $G_{\text{ref}}$  has  $m$  poles at zero. Then,  $G_{\text{ref}}$  can be written as

$$G_{\text{ref}}(z) = \frac{1}{z^m} G_{\text{ref},0}(z), \tag{20}$$

where  $G_{\text{ref},0}$  has no poles at zero. Note that the factor  $\frac{1}{z^m}$  shifts the indices of the power series coefficients of (20), but otherwise leaves them unchanged. Applying the above argument for  $G_{\text{ref},0}$  thus yields  $\rho(G) \leq 1$ . ■

The following result shows that there is a unique maximal annulus for which the coefficients of the Laurent series of  $G$  are bounded.

**Theorem 4.1:** *Let  $\rho_2 > \rho_1 \geq 0$ , and assume that  $\mathbb{A}(\rho_1, \rho_2)$  is maximal with respect to  $G$ . Then, the following statements are equivalent:*

- (i) *The coefficients of the Laurent series of  $G$  in  $\mathbb{A}(\rho_1, \rho_2)$  are square summable.*
- (ii) *The coefficients of the Laurent series of  $G$  in  $\mathbb{A}(\rho_1, \rho_2)$  converge to zero.*
- (iii) *The coefficients of the Laurent series of  $G$  in  $\mathbb{A}(\rho_1, \rho_2)$  are bounded.*
- (iv)  *$\rho_1 < 1 < \rho_2$ .*

**Proof:** (i) implies (ii) and (ii) implies (iii) are immediate. To show that (iii) implies (iv), assume that the coefficients of the Laurent series of  $G$  in  $\mathbb{A}(\rho_1, \rho_2)$  are bounded. Decompose  $G$  as  $G = G_i + G_o + D$ , where all of the poles of  $G_i$  are contained in  $\mathbb{D}(\rho_1)$  and all of the poles of  $G_o$  are contained in  $\mathbb{P}(\rho_2)$ . Suppose  $\rho_1 < \rho_2 < 1$  and  $\mathbb{A}(\rho_1, \rho_2)$  is maximal. Then,  $\rho_{\text{inner}}(G_o) < 1$ , and thus (i) of Lemma 4.1 implies that the coefficients of the Laurent series of  $G_o$ , and thus the coefficients of the Laurent series of  $G$ , are unbounded. Now suppose that  $1 < \rho_1 < \rho_2$  and  $\mathbb{A}(\rho_1, \rho_2)$  is maximal. Then,  $\rho(G_i) > 1$ , and thus (ii) of Lemma 4.1 implies that the coefficients of the Laurent series of  $G_i$ , and thus  $G$ , are unbounded. Therefore,  $\rho_1 < 1 < \rho_2$ .

To show that (iv) implies (i) assume that  $\rho_1 < 1 < \rho_2$  and consider the Laurent series of  $G$  in  $\mathbb{A}(\rho_1, \rho_2)$  given by (14), where  $\{L_i\}_{i=-\infty}^{\infty}$  is given by (15). Then,  $f : [0, \infty) \rightarrow \mathbb{C}$  defined by  $f(\theta) \triangleq G(e^{j\theta})$  is continuous and periodic. By Parseval's theorem, the coefficients of the Fourier series of  $f$  are square summable. Since, on the unit circle, the Laurent series of  $G$  given by (14) is identical to

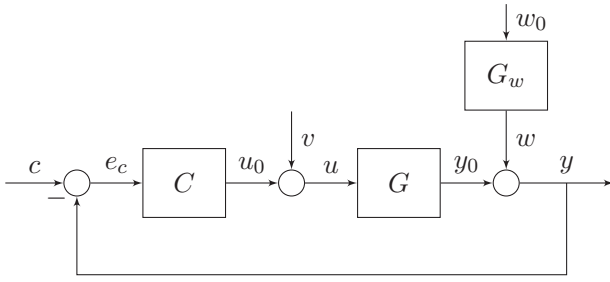


**Figure 1.** Discrete-time closed-loop control system, where  $C$  is the controller,  $G$  is the plant,  $v$  and  $w_0$  are white noise signals, and  $G_w$  is the output noise model. The plant  $G$  may be unstable, and the closed-loop system is assumed to be internally stable.

the Fourier series of  $f$ , it follows that  $\{L_i\}_{i=-\infty}^{\infty}$  is square summable. ■

**Theorem 4.1** applies to rational functions that have no poles on the unit circle. If this is not the case, let  $\rho_s < \alpha < 1$  be such that  $G$  has no poles on the circle  $|z| = \alpha$ . Consider the decomposition

$$G = G_{i,\alpha} + G_{o,\alpha} + D, \quad (21)$$

where all poles of  $G_{i,\alpha}$  are contained in  $\mathbb{D}(\alpha)$ , all poles of  $G_{o,\alpha}$  are contained in  $\mathbb{P}(\alpha)$ , and  $D = G(\infty)$ . Using (14), we have

$$\begin{aligned} G_\alpha(z) &\triangleq G(\alpha z) = \sum_{i=-\infty}^{\infty} L_i(\alpha z)^{-i} = \sum_{i=-\infty}^{\infty} \alpha^{-i} L_i z^{-i} \\ &= \sum_{i=-\infty}^{\infty} L_{\alpha,i} z^{-i}, \end{aligned} \quad (22)$$

where, for all  $i$ ,

$$L_{\alpha,i} \triangleq \alpha^{-i} L_i. \quad (23)$$

Let  $\rho_s < \alpha < 1$ , and assume that  $G$  has no poles on the circle  $|z| = \alpha$ . Therefore,  $G_\alpha$  has no poles on the unit circle. **Theorem 4.1** can now be applied to  $G_\alpha$  in  $\mathbb{A}(\frac{\rho_s}{\alpha}, \frac{\rho_u}{\alpha})$  and (23) can be used to compute the coefficients of the Laurent series of  $G$  in  $\mathbb{A}(\rho_s, \rho_u)$ .

## 5. Noncausal closed-loop identification

Consider the closed-loop system in **Figure 1** consisting of the MIMO, discrete-time transfer function  $G$  of order  $n$  and the discrete-time controller  $C$ . We assume that the closed-loop system is internally asymptotically stable, although no assumptions are made about the stability of  $G$  except that  $G$  has no poles on the unit circle. However, this restriction can be avoided by using (22).

Using the Laurent series (14) of  $G$  in  $\mathbb{A}(\rho_s, \rho_u)$ , the output of  $G$  can be written as

$$y_0(k) = \sum_{j=-\infty}^k L_j u(k-j), \quad (24)$$

where  $u(k) = 0$  for all  $k < 0$ . Note that the terms corresponding to  $j < 0$  represent the noncausal component of the model. Thus, for all  $k \geq 0$ , (24) can be represented as

$$y_0(k) = y_{0,r,d}(k) + e_{r,d}(k), \quad (25)$$

where the noncausal FIR model output  $y_{0,r,d}(k)$  is defined as

$$y_{0,r,d}(k) \triangleq \sum_{j=-d}^{\min\{r,k\}} L_j u(k-j), \quad (26)$$

and the *output error* at time  $k$  is defined by

$$e_{r,d}(k) \triangleq y_0(k) - y_{0,r,d}(k), \quad (27)$$

which is the difference between the true output and the noncausal FIR model output at time  $k$ . Using (24) and (26) it follows that, for all  $k \geq 0$ ,

$$\lim_{r,d \rightarrow \infty} y_{0,r,d}(k) = \sum_{j=-\infty}^k L_j u(k-j) = y_0(k). \quad (28)$$

Therefore, for all  $k \geq 0$ ,

$$\lim_{r,d \rightarrow \infty} e_{r,d}(k) = y_0(k) - \lim_{r,d \rightarrow \infty} y_{0,r,d}(k) = 0. \quad (29)$$

It follows from (26) that computing the output at time  $k$  requires the inputs  $u(k-r), \dots, u(k+d)$ . That is, to identify a noncausal FIR model, we delay the measured output data by  $d$  steps and then perform identification between the input and delayed output, as we show next.

Let  $c$ ,  $v$ , and  $w_0$  be realisations of the zero-mean stationary white random processes  $\mathcal{C}$ ,  $\mathcal{V}$ , and  $\mathcal{W}_0$ , respectively, and let  $w$  be a realisation of the stationary coloured random process  $\mathcal{W}$ . We assume that  $\mathcal{C}$ ,  $\mathcal{W}_0$ , and  $\mathcal{V}$  are mutually independent and ergodic, that is, their statistical properties can be determined from a single, sufficiently long realisation.

Let  $u$  and  $y$  denote measurements of the input  $u_0$  and output  $y_0$ , respectively, that is, for all  $k \geq 0$ ,

$$u(k) = u_0(k) + v(k), \quad (30)$$

$$y(k) = y_0(k) + w(k). \quad (31)$$

Note that (25) can be expressed as

$$y_0(k) = \theta_{r,d} \phi_{r,d}(k) + e_{r,d}(k), \quad (32)$$

where

$$\theta_{r,d} \triangleq [L_{-d} \cdots L_r], \quad \phi_{r,d}(k) \triangleq [u(k+d) \cdots u(k-r)]^T.$$

Moreover, for all  $k \geq 0$

$$y(k) = \theta_{r,d} \phi_{r,d}(k) + w(k) + e_{r,d}(k). \quad (33)$$

### 5.1 Noncausal closed-loop identification using least squares

The least squares (LS) estimate  $\hat{\theta}_{r,d}^{\text{LS}}$  of  $\theta_{r,d}$  is given by

$$\hat{\theta}_{r,d}^{\text{LS}} = \arg \min_{\bar{\theta}_{r,d}} \|\Psi_{y,\ell} - \bar{\theta}_{r,d} \Phi_{\mu,\ell}\|_{\text{F}}, \quad (34)$$

where  $\bar{\theta}_{r,d} \in \mathbb{R}^{l \times \mu m}$ ,

$$\begin{aligned} \Psi_{y,\ell} &\triangleq [y(r) \cdots y(\ell-d)], \\ \Phi_{\mu,\ell} &\triangleq [\phi_{r,d}(r) \cdots \phi_{r,d}(\ell-d)], \end{aligned}$$

$\mu \triangleq r + d + 1$ , and  $\ell$  is the number of samples. It follows from (34) that the least squares estimate  $\hat{\theta}_{r,d}^{\text{LS}}$  of  $\theta_{r,d}$  satisfies

$$\Psi_{y,\ell} \Phi_{\mu,\ell}^T = \hat{\theta}_{r,d}^{\text{LS}} \Phi_{\mu,\ell} \Phi_{\mu,\ell}^T. \quad (35)$$

Note that

$$\begin{aligned} \Psi_{y,\ell} &= \Psi_{y_0,\ell} + \Psi_{w,\ell}, & \Psi_{y_0,\ell} &= \theta_{r,d} \Phi_{\mu,\ell} + \Psi_{e_{r,d},\ell}, \\ \Phi_{\mu,\ell} &= \Phi_{\mu_0,\ell} + \Phi_{v,\ell}, \end{aligned} \quad (36)$$

where

$$\begin{aligned} \Psi_{y_0,\ell} &\triangleq [y_0(r) \cdots y_0(\ell-d)], \\ \Psi_{w,\ell} &\triangleq [w(r) \cdots w(\ell-d)], \\ \Phi_{\mu_0,\ell} &\triangleq [\phi_{0,r,d}(r) \cdots \phi_{0,r,d}(\ell-d)], \\ \phi_{0,r,d}(k) &\triangleq [u_0(k+d) \cdots u_0(k-r)]^T, \\ \Phi_{v,\ell} &\triangleq [\phi_{v,r,d}(r) \cdots \phi_{v,r,d}(\ell-d)], \\ \phi_{v,r,d}(k) &\triangleq [v(k+d) \cdots v(k-r)]^T. \end{aligned}$$

Then, (35) becomes

$$\theta_{r,d} \Phi_{\mu,\ell} \Phi_{\mu,\ell}^T + \Psi_{w,\ell} \Phi_{\mu,\ell}^T + \Psi_{e_{r,d},\ell} \Phi_{\mu,\ell}^T = \hat{\theta}_{r,d}^{\text{LS}} \Phi_{\mu,\ell} \Phi_{\mu,\ell}^T, \quad (37)$$

where

$$\Psi_{e_{r,d},\ell} \triangleq [e_{r,d}(r) \cdots e_{r,d}(\ell-d)].$$

Note from Figure 1 that  $u$  can be written as

$$u(k) = G_{u,c}(z)c(k) + G_{u,v}(z)v(k) + G_{u,w_0}(z)w_0(k), \quad (38)$$

where  $G_{u,c}$ ,  $G_{u,v}$ , and  $G_{u,w_0}$  are the asymptotically stable closed-loop transfer functions from  $c$ ,  $v$ , and  $w_0$  to  $u$ , respectively. It follows from (38) that we can write

$$\mathcal{U}(k) = G_{u,c}(z)\mathcal{C}(k) + G_{u,v}(z)\mathcal{V}(k) + G_{u,w_0}(z)\mathcal{W}_0(k). \quad (39)$$

Since  $\mathcal{C}$ ,  $\mathcal{V}$ , and  $\mathcal{W}_0$  are ergodic processes and  $\mathcal{U}$  is the output of a linear time-invariance (LTI) system whose inputs are ergodic, then (39) implies that  $\mathcal{U}$  is also ergodic. Similarly, we can show that  $\mathcal{W}$ ,  $\mathcal{Y}_0$ , and  $\mathcal{Y}$  are ergodic.

Dividing (37) by  $\ell$  and taking the limit as  $\ell$  tends to infinity yields

$$\begin{aligned} \theta_{r,d} \lim_{\ell \rightarrow \infty} \frac{1}{\ell} \Phi_{\mu,\ell} \Phi_{\mu,\ell}^T + \lim_{\ell \rightarrow \infty} \frac{1}{\ell} \Psi_{w,\ell} \Phi_{\mu,\ell}^T + \lim_{\ell \rightarrow \infty} \frac{1}{\ell} \Psi_{e_{r,d},\ell} \Phi_{\mu,\ell}^T \\ \stackrel{\text{wpl}}{=} \lim_{\ell \rightarrow \infty} \frac{1}{\ell} \hat{\theta}_{r,d}^{\text{LS}} \Phi_{\mu,\ell} \Phi_{\mu,\ell}^T, \end{aligned} \quad (40)$$

where  $\lim_{\ell \rightarrow \infty} \frac{1}{\ell} \Phi_{\mu,\ell} \Phi_{\mu,\ell}^T$ ,  $\lim_{\ell \rightarrow \infty} \frac{1}{\ell} \Psi_{w,\ell} \Phi_{\mu,\ell}^T$ , and  $\lim_{\ell \rightarrow \infty} \frac{1}{\ell} \Psi_{e_{r,d},\ell} \Phi_{\mu,\ell}^T$  exist due to ergodicity conditions.

Define

$$Q \triangleq \lim_{\ell \rightarrow \infty} \frac{1}{\ell} \Phi_{\mu,\ell} \Phi_{\mu,\ell}^T. \quad (41)$$

Therefore, (40) can be written as

$$\theta_{r,d} Q + \lim_{\ell \rightarrow \infty} \frac{1}{\ell} \Psi_{w,\ell} \Phi_{\mu,\ell}^T + \lim_{\ell \rightarrow \infty} \frac{1}{\ell} \Psi_{e_{r,d},\ell} \Phi_{\mu,\ell}^T \stackrel{\text{wpl}}{=} \lim_{\ell \rightarrow \infty} \hat{\theta}_{r,d}^{\text{LS}} Q. \quad (42)$$

Taking the limit as  $r$  and  $d$  tend to infinity, (42) becomes

$$\begin{aligned} \lim_{r,d \rightarrow \infty} \theta_{r,d} Q + \lim_{r,d \rightarrow \infty} \lim_{\ell \rightarrow \infty} \frac{1}{\ell} \Psi_{w,\ell} \Phi_{\mu,\ell}^T \\ + \lim_{r,d \rightarrow \infty} \lim_{\ell \rightarrow \infty} \frac{1}{\ell} \Psi_{e_{r,d},\ell} \Phi_{\mu,\ell}^T \stackrel{\text{wpl}}{=} \lim_{r,d \rightarrow \infty} \lim_{\ell \rightarrow \infty} \hat{\theta}_{r,d}^{\text{LS}} Q. \end{aligned} \quad (43)$$

It follows from (29) that

$$\lim_{r,d \rightarrow \infty} \lim_{\ell \rightarrow \infty} \frac{1}{\ell} \Psi_{e_{r,d},\ell} \Phi_{\mu,\ell}^T \stackrel{\text{wpl}}{=} 0_{l \times \mu m}. \quad (44)$$

Therefore, (43) becomes

$$\lim_{r,d \rightarrow \infty} \lim_{\ell \rightarrow \infty} \frac{1}{\ell} \Psi_{w,\ell} \Phi_{\mu,\ell}^T \stackrel{\text{wp1}}{=} \left( \lim_{r,d \rightarrow \infty} \lim_{\ell \rightarrow \infty} \hat{\theta}_{r,d,\ell}^{\text{LS}} - \lim_{r,d \rightarrow \infty} \theta_{r,d} \right) Q. \quad (45)$$

Since  $w$  and  $u$  are realisations of correlated processes, it follows that  $\lim_{r,d \rightarrow \infty} \lim_{\ell \rightarrow \infty} \frac{1}{\ell} \Psi_{w,\ell} \Phi_{\mu,\ell}^T$  is not zero. Therefore, (45) implies that  $(\lim_{r,d \rightarrow \infty} \lim_{\ell \rightarrow \infty} \hat{\theta}_{r,d,\ell}^{\text{LS}} - \lim_{r,d \rightarrow \infty} \theta_{r,d})Q$  is not zero, which implies that  $\lim_{r,d \rightarrow \infty} \lim_{\ell \rightarrow \infty} \hat{\theta}_{r,d,\ell}^{\text{LS}} - \lim_{r,d \rightarrow \infty} \theta_{r,d}$  is not in the left null space of  $Q$ , and thus is not zero. Therefore,  $\hat{\theta}_{r,d,\ell}^{\text{LS}}$  is not a consistent estimator of  $\theta_{r,d}$ .

## 5.2 Noncausal closed-loop identification using the instrumental variables method

The basic instrumental variables (BIV) method (Söderström & Stoica, 2002) is used with an FIR model to identify the transfer function  $G$  shown in Figure 1 by modifying (35) (Söderström & Stoica, 1983, 2002). A typical choice of the vector of instrumental variables for closed-loop identification is to use samples of the command signal  $c$  (Gilson & Van den Hof, 2005). Let  $\phi_{c,r,d}(k)$  denote the vector of instrumental variables, that is,

$$\phi_{c,r,d}(k) \triangleq [c(k+d) \cdots c(k-r)]^T \in \mathbb{R}^{\mu m}. \quad (46)$$

We then modify (35) as

$$\Psi_{y,\ell} \Phi_{c,\mu,\ell}^T = \hat{\theta}_{r,d,\ell}^{\text{IV}} \Phi_{\mu,\ell} \Phi_{c,\mu,\ell}^T, \quad (47)$$

where

$$\Phi_{c,\mu,\ell} \triangleq [\phi_{c,r,d}(r) \cdots \phi_{c,r,d}(\ell-d)]. \quad (48)$$

Then, (47) becomes

$$\begin{aligned} \theta_{r,d} \Phi_{\mu_0,\ell} \Phi_{c,\mu,\ell}^T + \theta_{r,d} \Phi_{v,\ell} \Phi_{c,\mu,\ell}^T + \Psi_{w,\ell} \Phi_{c,\mu,\ell}^T \\ + \Psi_{e_{r,d,\ell}} \Phi_{c,\mu,\ell}^T = \hat{\theta}_{r,d,\ell}^{\text{IV}} \Phi_{\mu_0,\ell} \Phi_{c,\mu,\ell}^T + \hat{\theta}_{r,d,\ell}^{\text{IV}} \Phi_{v,\ell} \Phi_{c,\mu,\ell}^T. \end{aligned} \quad (49)$$

Since  $\mathcal{C}$ ,  $\mathcal{W}_0$ , and  $\mathcal{V}$  are ergodic processes, (49) implies

$$\begin{aligned} \theta_{r,d} \lim_{\ell \rightarrow \infty} \frac{1}{\ell} \Phi_{\mu_0,\ell} \Phi_{c,\mu,\ell}^T + \theta_{r,d} \lim_{\ell \rightarrow \infty} \frac{1}{\ell} \Phi_{v,\ell} \Phi_{c,\mu,\ell}^T \\ + \lim_{\ell \rightarrow \infty} \frac{1}{\ell} \Psi_{w,\ell} \Phi_{c,\mu,\ell}^T + \lim_{\ell \rightarrow \infty} \frac{1}{\ell} \Psi_{e_{r,d,\ell}} \Phi_{c,\mu,\ell}^T \\ \stackrel{\text{wp1}}{=} \lim_{\ell \rightarrow \infty} \frac{1}{\ell} \hat{\theta}_{r,d,\ell}^{\text{IV}} \Phi_{\mu_0,\ell} \Phi_{c,\mu,\ell}^T + \lim_{\ell \rightarrow \infty} \frac{1}{\ell} \hat{\theta}_{r,d,\ell}^{\text{IV}} \Phi_{v,\ell} \Phi_{c,\mu,\ell}^T. \end{aligned} \quad (50)$$

Using (50), consistency of the estimated Markov parameters holds if  $\Phi_{c,\mu,\ell}$  satisfies the following assumptions:

$$(A1) \lim_{\ell \rightarrow \infty} \frac{1}{\ell} \Phi_{\mu_0,\ell} \Phi_{c,\mu,\ell}^T \text{ is nonsingular.}$$

$$(A2) \lim_{\ell \rightarrow \infty} \frac{1}{\ell} \Psi_{w,\ell} \Phi_{c,\mu,\ell}^T \stackrel{\text{wp1}}{=} 0_{l \times \mu m}.$$

$$(A3) \lim_{\ell \rightarrow \infty} \frac{1}{\ell} \Phi_{v,\ell} \Phi_{c,\mu,\ell}^T \stackrel{\text{wp1}}{=} 0_{\mu m \times \mu m}.$$

The vector of instrumental variables is constructed from the command signal data, which is a realisation of a stationary white random process and satisfies (A1) (Gilson & Van den Hof, 2005). Next, note that

$$\begin{aligned} \lim_{\ell \rightarrow \infty} \frac{1}{\ell} \Psi_{w,\ell} \Phi_{c,\mu,\ell}^T &= \lim_{\ell \rightarrow \infty} \frac{1}{\ell} [w(r) \cdots w(\ell-d)] \\ &\times \begin{bmatrix} c(r+d) & \cdots & c(0) \\ \vdots & \cdots & \vdots \\ c(\ell) & \cdots & c(\ell-r-d) \end{bmatrix} \\ &= \lim_{\ell \rightarrow \infty} \frac{1}{\ell} \left[ \sum_{i=r}^{\ell-d} w(i)c(i+d) \cdots \sum_{i=r}^{\ell-d} w(i)c(r-i) \right] \\ &\stackrel{\text{wp1}}{=} [\mathbb{E}[\mathcal{W}(k)\mathcal{C}(k+d)] \cdots \mathbb{E}[\mathcal{W}(k)\mathcal{C}(r-k)]] = 0_{l \times \mu m}, \end{aligned} \quad (51)$$

where the last equality follows from the assumptions that  $\mathcal{W}$  and  $\mathcal{C}$  are independent processes and  $\mathcal{C}$  is zero-mean. Similarly, we can show that

$$\lim_{\ell \rightarrow \infty} \frac{1}{\ell} \Phi_{v,\ell} \Phi_{c,\mu,\ell}^T = 0_{\mu m \times \mu m}. \quad (52)$$

Then, it follows from (51) and (52) that the choice of the instrumental variables satisfies (A2) and (A3). Moreover, using (51) and (52), (50) becomes

$$\begin{aligned} \theta_{r,d} \left[ \lim_{\ell \rightarrow \infty} \frac{1}{\ell} \Phi_{\mu_0,\ell} \Phi_{c,\mu,\ell}^T \right] + \lim_{\ell \rightarrow \infty} \frac{1}{\ell} \Psi_{e_{r,d,\ell}} \Phi_{c,\mu,\ell}^T \\ \stackrel{\text{wp1}}{=} \lim_{\ell \rightarrow \infty} \hat{\theta}_{r,d,\ell}^{\text{IV}} \left[ \lim_{\ell \rightarrow \infty} \frac{1}{\ell} \Phi_{\mu_0,\ell} \Phi_{c,\mu,\ell}^T \right]. \end{aligned} \quad (53)$$

Taking the limit of (53) as  $r$  and  $d$  tend to infinity and using (44) and assumption (A1), (53) becomes

$$\lim_{r,d \rightarrow \infty} \lim_{\ell \rightarrow \infty} \hat{\theta}_{r,d,\ell}^{\text{IV}} \stackrel{\text{wp1}}{=} \lim_{r,d \rightarrow \infty} \theta_{r,d}. \quad (54)$$

We choose  $r$  and  $d$  to be sufficiently large such that  $\lim_{\ell \rightarrow \infty} \frac{1}{\ell} \Psi_{e_{r,d,\ell}} \Phi_{c,\mu,\ell}^T$  is negligible.

The extended instrumental variables (XIV) method generalises the basic instrumental variables method by prefiltering the sampled data of the instrumental variables (Gilson & Van den Hof, 2005; Söderström & Stoica, 2002). That is, in (47), we replace  $\Phi_{c,\mu,\ell}$  by

$$\Phi_{\tilde{c},\mu,\ell} \triangleq L(z) \Phi_{c,\mu,\ell}, \quad (55)$$

where  $L(z)$  is an asymptotically stable filter. Using the same argument used above to show consistency for the basic instrumental variables method, consistency of the estimated Markov parameters of XIV denoted by  $\hat{\theta}_{r,d,\ell}^{\text{XIV}}$  holds if  $\Phi_{\hat{c},\mu,\ell}$  satisfies the assumptions

$$(B1) \lim_{\ell \rightarrow \infty} \frac{1}{\ell} \Phi_{\mu_0,\ell} \Phi_{\hat{c},\mu,\ell}^T \text{ is nonsingular.}$$

$$(B2) \lim_{\ell \rightarrow \infty} \frac{1}{\ell} \Psi_{w,\ell} \Phi_{\hat{c},\mu,\ell}^T \stackrel{\text{wp1}}{=} 0_{l \times \mu m}.$$

$$(B3) \lim_{\ell \rightarrow \infty} \frac{1}{\ell} \Phi_{v,\ell} \Phi_{\hat{c},\mu,\ell}^T \stackrel{\text{wp1}}{=} 0_{\mu m \times \mu m}.$$

### 5.3 Noncausal closed-loop identification using prediction error methods

Let  $\hat{G}_\ell(\mathbf{q})$  and  $\hat{G}_{w,\ell}(\mathbf{q})$  be estimates of  $G(\mathbf{q})$  and  $G_w(\mathbf{q})$ , respectively, obtained with  $\ell$  samples of input and output data, and assume that  $G_w(\mathbf{q})$  and  $\hat{G}_{w,\ell}(\mathbf{q})$  are square and nonsingular. Note that  $y$  in Figure 1 can be written as

$$y(k) = G(\mathbf{q})u(k) + G_w(\mathbf{q})w_0(k). \quad (56)$$

Then, the one-step predictor of (56) is defined by Ljung (1999)

$$y(k|\hat{G}_\ell, \hat{G}_{w,\ell}) \triangleq \hat{G}_{w,\ell}^{-1}(\mathbf{q})\hat{G}_\ell(\mathbf{q})u(k) + (1 - \hat{G}_{w,\ell}^{-1}(\mathbf{q}))y(k). \quad (57)$$

Define the prediction error

$$\varepsilon(k|\hat{G}_\ell, \hat{G}_{w,\ell}) \triangleq y(k) - y(k|\hat{G}_\ell, \hat{G}_{w,\ell}). \quad (58)$$

Using (56) and (57), (58) can be written as

$$\begin{aligned} \varepsilon(k|\hat{G}_\ell, \hat{G}_{w,\ell}) &= y(k) - \hat{G}_{w,\ell}^{-1}(\mathbf{q})\hat{G}_\ell(\mathbf{q})u(k) \\ &\quad - (1 - \hat{G}_{w,\ell}^{-1}(\mathbf{q}))y(k) \\ &= \hat{G}_{w,\ell}^{-1}(\mathbf{q})(y(k) - \hat{G}_\ell(\mathbf{q})u(k)) \\ &= \hat{G}_{w,\ell}^{-1}(\mathbf{q})((G(\mathbf{q}) - \hat{G}_\ell(\mathbf{q}))u(k) \\ &\quad + G_w(\mathbf{q})w_0(k)) \\ &= \hat{G}_{w,\ell}^{-1}(\mathbf{q})((G(\mathbf{q}) - \hat{G}_\ell(\mathbf{q}))u(k) \\ &\quad + (G_w(\mathbf{q}) - \hat{G}_{w,\ell}(\mathbf{q}))w_0(k)) + w_0(k). \end{aligned} \quad (59)$$

Assume that  $G$ ,  $G_w$ , and  $G_w^{-1}$  have no poles on the unit circle. Then  $G$ ,  $G_w$ , and  $G_w^{-1}$  are analytic in the maximal annulus that contains the unit circle with the Laurent series given by (14) for  $G$  and with the Laurent series

$$G_w(z) = \sum_{i=-\infty}^{\infty} M_i z^{-i}, \quad (60)$$

$$G_w^{-1}(z) = \sum_{i=-\infty}^{\infty} N_i z^{-i}, \quad (61)$$

for  $G_w$  and  $G_w^{-1}$ , respectively, in the maximal annulus that contains the unit circle, where for all  $i$ ,  $M_i$ ,  $N_i \in \mathbb{R}^{l \times l}$ . Define

$$\begin{aligned} \mathcal{H}(\mathbf{q}, \theta_{r,d}) &\triangleq \sum_{i=-d}^r L_i \mathbf{q}^{-i}, \quad \mathcal{H}(\mathbf{q}, \theta_{M,r,d}) \triangleq \sum_{i=-d}^r M_i \mathbf{q}^{-i}, \\ \mathcal{H}(\mathbf{q}, \theta_{N,r,d}) &\triangleq \sum_{i=-d}^r N_i \mathbf{q}^{-i}, \\ \theta_{r,d} &\triangleq [L_{-d} \cdots L_r], \quad \theta_{M,r,d} \triangleq [M_{-d} \cdots M_r], \\ \theta_{N,r,d} &\triangleq [N_{-d} \cdots N_r], \end{aligned} \quad (62)$$

where  $\theta_{r,d} \in \mathbb{R}^{l \times \mu m}$ , and  $\theta_{M,r,d}, \theta_{N,r,d} \in \mathbb{R}^{l \times \mu l}$ . Note from (26) and (62) that

$$y_{0,r,d}(k) = \mathcal{H}(\mathbf{q}, \theta_{r,d})u(k). \quad (64)$$

Therefore, (27) implies that

$$\begin{aligned} e_{r,d}(k) &= y_0(k) - \mathcal{H}(\mathbf{q}, \theta_{r,d})u(k) \\ &= G(\mathbf{q})u(k) - \mathcal{H}(\mathbf{q}, \theta_{r,d})u(k). \end{aligned} \quad (65)$$

Moreover, define

$$\begin{aligned} e_{w,r,d}(k) &\triangleq w(k) - \mathcal{H}(\mathbf{q}, \theta_{M,r,d})w_0(k) \\ &= G_w(\mathbf{q})w_0(k) - \mathcal{H}(\mathbf{q}, \theta_{M,r,d})w_0(k). \end{aligned} \quad (66)$$

Therefore, (65) and (66) imply, respectively, that

$$G(\mathbf{q})u(k) = \mathcal{H}(\mathbf{q}, \theta_{r,d})u(k) + e_{r,d}(k), \quad (67)$$

$$G_w(\mathbf{q})w_0(k) = \mathcal{H}(\mathbf{q}, \theta_{M,r,d})w_0(k) + e_{w,r,d}(k). \quad (68)$$

Let

$$\begin{aligned} \mathcal{H}(\mathbf{q}, \hat{\theta}_{r,d,\ell}) &\triangleq \hat{G}_\ell(\mathbf{q}) = \sum_{i=-d}^r \hat{L}_{i,\ell} \mathbf{q}^{-i}, \\ \hat{\theta}_{r,d,\ell} &\triangleq [\hat{L}_{-d,\ell} \cdots \hat{L}_{r,\ell}], \end{aligned} \quad (69)$$

$$\begin{aligned} \mathcal{H}(\mathbf{q}, \hat{\theta}_{M,r,d,\ell}) &\triangleq \hat{G}_{w,\ell}(\mathbf{q}) = \sum_{i=-d}^r \hat{M}_{i,\ell} \mathbf{q}^{-i}, \\ \hat{\theta}_{M,r,d,\ell} &\triangleq [\hat{M}_{-d,\ell} \cdots \hat{M}_{r,\ell}], \end{aligned} \quad (70)$$

$$\begin{aligned} \mathcal{H}(\mathbf{q}, \hat{\theta}_{N,r,d,\ell}) &\triangleq \hat{G}_{w,\ell}^{-1}(\mathbf{q}) = \sum_{i=-d}^r \hat{N}_{i,\ell} \mathbf{q}^{-i}, \\ \hat{\theta}_{N,r,d,\ell} &\triangleq [\hat{N}_{-d,\ell} \cdots \hat{N}_{r,\ell}], \end{aligned} \quad (71)$$

where  $\hat{\theta}_{r,d,\ell} \in \mathbb{R}^{l \times \mu m}$  and  $\hat{\theta}_{M,r,d,\ell}, \hat{\theta}_{N,r,d,\ell} \in \mathbb{R}^{l \times \mu l}$ . Then, using (67)–(71), (59) can be rewritten as

$$\begin{aligned} \varepsilon(k|\hat{\theta}_{r,d,\ell}, \hat{\theta}_{M,r,d,\ell}, \hat{\theta}_{N,r,d,\ell}) &\triangleq \mathcal{H}(\mathbf{q}, \hat{\theta}_{N,r,d,\ell}) \\ &\times [(\mathcal{H}(\mathbf{q}, \theta_{r,d}) - \mathcal{H}(\mathbf{q}, \hat{\theta}_{r,d,\ell}))u(k) \\ &+ (\mathcal{H}(\mathbf{q}, \theta_{M,r,d}) - \mathcal{H}(\mathbf{q}, \hat{\theta}_{M,r,d,\ell}))w_0(k) \\ &+ e_{r,d}(k) + e_{w,r,d}(k)] + w_0(k) \\ &= \mathcal{H}(\mathbf{q}, \hat{\theta}_{N,r,d,\ell})[T^T(\mathbf{q}, \hat{\theta}_{r,d,\ell}, \hat{\theta}_{M,r,d,\ell})\xi(k) \\ &+ e_{r,d}(k) + e_{w,r,d}(k)] + w_0(k), \end{aligned} \quad (72)$$

where

$$\begin{aligned} T(\mathbf{q}, \hat{\theta}_{r,d,\ell}, \hat{\theta}_{M,r,d,\ell}) &\triangleq \begin{bmatrix} \mathcal{H}(\mathbf{q}, \theta_{r,d}) - \mathcal{H}(\mathbf{q}, \hat{\theta}_{r,d,\ell}) \\ \mathcal{H}(\mathbf{q}, \theta_{M,r,d}) - \mathcal{H}(\mathbf{q}, \hat{\theta}_{M,r,d,\ell}) \end{bmatrix}, \\ \xi(k) &\triangleq \begin{bmatrix} u(k) \\ w_0(k) \end{bmatrix}. \end{aligned} \quad (73)$$

Define

$$\hat{\theta}_\ell \triangleq \lim_{r,d \rightarrow \infty} \hat{\theta}_{r,d,\ell}, \quad \hat{\theta}_{M,\ell} \triangleq \lim_{r,d \rightarrow \infty} \hat{\theta}_{M,r,d,\ell}, \quad \hat{\theta}_{N,\ell} \triangleq \lim_{r,d \rightarrow \infty} \hat{\theta}_{N,r,d,\ell}, \quad (74)$$

$$\varepsilon(k|\hat{\theta}_\ell, \hat{\theta}_{M,\ell}, \hat{\theta}_{N,\ell}) \triangleq \lim_{r,d \rightarrow \infty} \varepsilon(k|\hat{\theta}_{r,d,\ell}, \hat{\theta}_{M,r,d,\ell}, \hat{\theta}_{N,r,d,\ell}), \quad (75)$$

$$\begin{aligned} T(\mathbf{q}, \hat{\theta}, \hat{\theta}_{M,\ell}) &\triangleq \lim_{r,d \rightarrow \infty} T(\mathbf{q}, \hat{\theta}_{r,d,\ell}, \hat{\theta}_{M,r,d,\ell}) \\ &= \begin{bmatrix} \mathcal{H}(\mathbf{q}, \theta) - \mathcal{H}(\mathbf{q}, \hat{\theta}_\ell) \\ \mathcal{H}(\mathbf{q}, \theta_M) - \mathcal{H}(\mathbf{q}, \hat{\theta}_{M,\ell}) \end{bmatrix}. \end{aligned} \quad (76)$$

Note from (60) and (62) that

$$\lim_{r,d \rightarrow \infty} \mathcal{H}(\mathbf{q}, \theta_{M,r,d}) = G_w(\mathbf{q}), \quad (77)$$

which implies that

$$\lim_{r,d \rightarrow \infty} e_{w,r,d}(k) = G_w(\mathbf{q})w_0(k) - \lim_{r,d \rightarrow \infty} \mathcal{H}(\mathbf{q}, \theta_{M,r,d})w_0(k) = 0. \quad (78)$$

Using (29) and (74)–(78), taking the limit of (72) as  $r$  and  $d$  tend to infinity yields

$$\varepsilon(k|\hat{\theta}_\ell, \hat{\theta}_{M,\ell}, \hat{\theta}_{N,\ell}) = \mathcal{H}(\mathbf{q}, \hat{\theta}_{N,\ell})T^T(\mathbf{q}, \hat{\theta}_\ell, \hat{\theta}_{M,\ell})\xi(k) + w_0(k). \quad (79)$$

Next, define the cost function

$$V(\ell, \hat{\theta}_\ell, \hat{\theta}_{M,\ell}, \hat{\theta}_{N,\ell}) \triangleq \frac{1}{\ell} \sum_{k=1}^{\ell} \|\varepsilon(k|\hat{\theta}_\ell, \hat{\theta}_{M,\ell}, \hat{\theta}_{N,\ell})\|_2^2. \quad (80)$$

Define

$$\hat{\theta} \triangleq \lim_{\ell \rightarrow \infty} \hat{\theta}_\ell, \quad \hat{\theta}_M \triangleq \lim_{\ell \rightarrow \infty} \hat{\theta}_{M,\ell}, \quad \hat{\theta}_N \triangleq \lim_{\ell \rightarrow \infty} \hat{\theta}_{N,\ell}, \quad (81)$$

which are independent of the data due to ergodicity. Define

$$\bar{V}(\hat{\theta}, \hat{\theta}_M, \hat{\theta}_N) \triangleq \lim_{\ell \rightarrow \infty} V(\ell, \hat{\theta}_\ell, \hat{\theta}_{M,\ell}, \hat{\theta}_{N,\ell}). \quad (82)$$

Using Parseval's theorem, (82) becomes

$$\bar{V}(\hat{\theta}, \hat{\theta}_M, \hat{\theta}_N) = \frac{1}{2\pi} \int_{-\pi}^{\pi} \Phi_\varepsilon(\omega) d\omega, \quad (83)$$

where using (79), the spectrum of  $\varepsilon$  is given by

$$\begin{aligned} \Phi_\varepsilon(\omega) &\triangleq \mathcal{H}(e^{j\omega}, \hat{\theta}_N)T^T(e^{j\omega}, \hat{\theta}, \hat{\theta}_M)\Phi_\xi(\omega)T(e^{-j\omega}, \hat{\theta}, \hat{\theta}_M) \\ &\times \mathcal{H}^T(e^{-j\omega}, \hat{\theta}_N) + \lambda_{w_0}, \end{aligned} \quad (84)$$

$\mathcal{H}(e^{j\omega}, \hat{\theta}_N)$  and  $T(e^{j\omega}, \hat{\theta}, \hat{\theta}_M)$  are the discrete-time Fourier transforms of  $\mathcal{H}(\mathbf{q}, \hat{\theta}_N)$  and  $T(\mathbf{q}, \hat{\theta}, \hat{\theta}_M)$ , respectively,

$$\Phi_\xi(\omega) \triangleq \begin{bmatrix} \Phi_u(\omega) & \Phi_{u,w_0}(\omega) \\ \Phi_{w_0,u}(\omega) & \lambda_{w_0} \end{bmatrix} \quad (85)$$

is the spectrum of  $\xi$ ,  $\Phi_u$  is the spectrum of  $u$ ,  $\lambda_{w_0}$  is the variance of  $w_0$ , and  $\Phi_{u,w_0}$  and  $\Phi_{w_0,u}$  are the cross-power spectra between  $u$  and  $w_0$ .

Note from (76) and (84) that  $T(e^{j\omega}, \hat{\theta}, \hat{\theta}_M) = T(e^{j\omega}, \theta, \theta_M)$  is the global minimiser of (84), which implies that the PEM estimates  $\hat{\theta}_\ell^{\text{PEM}}$  and  $\hat{\theta}_{M,\ell}^{\text{PEM}}$  of  $\theta$  and  $\theta_M$ , respectively, converge to the true values as  $\ell$  tends to infinity, that is,

$$\lim_{\ell \rightarrow \infty} \hat{\theta}_\ell^{\text{PEM}} = \theta, \quad \lim_{\ell \rightarrow \infty} \hat{\theta}_{M,\ell}^{\text{PEM}} = \theta_M. \quad (86)$$

We choose  $r$  and  $d$  to be sufficiently large such that  $e_{r,d}(k)$  and  $e_{w,r,d}(k)$  are negligible for all  $k \geq 1$ .

## 6. Numerical examples

In order to identify a noncausal FIR model of a transfer function  $G$  in the closed-loop system shown in Figure 1, we apply least squares, instrumental variables methods, and prediction error methods using input data and output data delayed by  $d$  steps. A nonzero estimate of the noncausal component of the identified FIR model indicates that  $G$  may have at least one unstable pole; otherwise  $G$  is asymptotically stable.

We assume that the command signal  $c$  in Figure 1 is a realisation of a stationary white random process  $\mathcal{C}$  with Gaussian probability density function  $\mathcal{N}(0, 1)$ . Moreover, we assume that the intermediate signal  $u$  is measured. In the first example in this section, we assume noise-free data, that is,  $v(k) = 0$  and  $w(k) = 0$  for all  $k \geq 0$ , and we use least squares to identify a noncausal FIR model of  $G$ . Then, we compare the coefficients of the identified noncausal FIR model of  $G$  to the coefficients of the Laurent series of  $G$  in the annulus that contains the unit circle. The second example compares the accuracy of the identified model obtained using least squares, instrumental variables methods, and prediction error methods for both IIR and noncausal FIR models in the presence of noise.

**Example 6.1:** Consider the unstable MIMO system

$$G(z) = \begin{bmatrix} G_{1,1}(z) & G_{1,2}(z) \\ G_{2,1}(z) & G_{2,2}(z) \end{bmatrix} \triangleq \frac{1}{z^2 - 2z + 0.35} \times \begin{bmatrix} -z + 6.3 & 5z - 11.9 \\ 4z - 14 & -12z + 26 \end{bmatrix}, \quad (87)$$

with the realisation

$$A = \begin{bmatrix} 1.5 & 0.2 \\ 2 & 0.5 \end{bmatrix}, \quad B = \begin{bmatrix} 1 & -1 \\ -1 & 3 \end{bmatrix}, \\ C = \begin{bmatrix} 1 & 2 \\ 0 & -4 \end{bmatrix}, \quad D = 0_{2 \times 2}. \quad (88)$$

Consider the LQR controller with  $Q = 2I_2$  and  $R = I_2$ , where  $I_2$  is the  $2 \times 2$  identity matrix,

and thus

$$K = \begin{bmatrix} 2.5446 & 0.4259 \\ 1.3095 & 0.2707 \end{bmatrix}. \quad (89)$$

Let  $r = d = 25$ . Figure 2 shows the Laurent series coefficients of  $G$  in  $\mathbb{A}(\rho_s, \rho_u)$ , where  $\rho_s \approx 0.1938$  and  $\rho_u \approx 1.8062$ . Figure 2 also shows the identified noncausal FIR model coefficients of  $G$  obtained using least squares. Note that the Laurent series of  $G$  has both causal and noncausal components, where the causal components are due to the asymptotically stable part of  $G$  and the noncausal components are due to the unstable part of  $G$ . Moreover, note that the coefficients of the Laurent series of  $G$  in  $\mathbb{A}(\rho_s, \rho_u)$  coincide with the coefficients of the identified noncausal FIR model of  $G$ .

**Example 6.2:** Consider the seventh-order unstable but not strongly unstable transfer function

$$G(z) = \frac{(z^2 + 0.16)(z - 0.3)(z + 0.3)}{(z + 0.7)(z + 0.6)(z^2 + 0.25)(z - 1.8)(z - 1.7)(z - 1.6)} \quad (90)$$

with the realisation

$$A = \begin{bmatrix} 3.800 & -2.7000 & -3.2700 & 2.1151 & 1.0013 & 0.6819 & 0.5141 \\ 1 & 0 & 0 & 0 & 0 & 0 & 0 \\ 0 & 1 & 0 & 0 & 0 & 0 & 0 \\ 0 & 0 & 1 & 0 & 0 & 0 & 0 \\ 0 & 0 & 0 & 1 & 0 & 0 & 0 \\ 0 & 0 & 0 & 0 & 1 & 0 & 0 \\ 0 & 0 & 0 & 0 & 0 & 1 & 0 \end{bmatrix}, \quad B = \begin{bmatrix} 1 \\ 0 \\ 0 \\ 0 \\ 0 \\ 0 \\ 0 \end{bmatrix}, \quad (91)$$

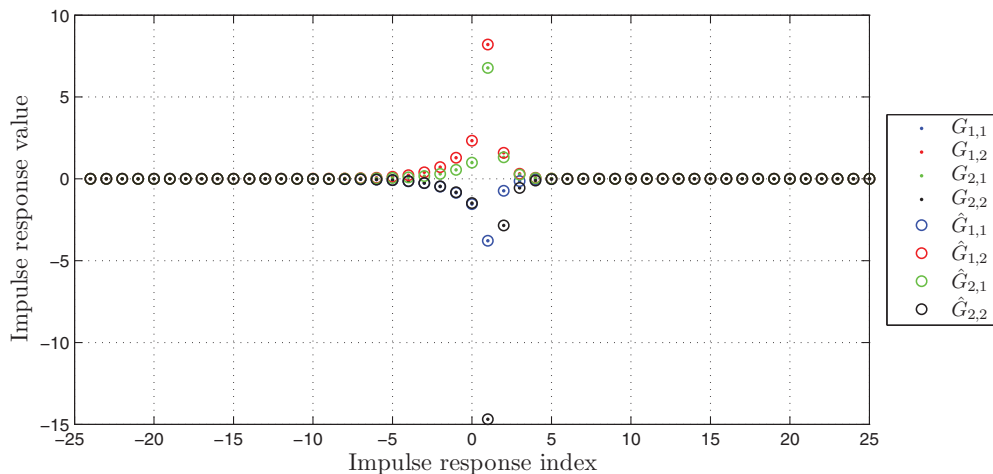


**Figure 2.**  $G$  is the MIMO system (87) and  $r = d = 25$ . The coefficients of the Laurent series of  $G$  are shown by dot markers, and the coefficients of the identified impulse response of  $G$  are shown by circle markers. Note that the Laurent series of  $G$  has both causal and noncausal components, where the causal components are due to the asymptotically stable part of  $G$  and the noncausal components are due to the unstable part of  $G$ . Moreover, note that the coefficients of the Laurent series of  $G$  in  $\mathbb{A}(\rho_s, \rho_u)$ , where  $\rho_s \approx 0.1938$  and  $\rho_u \approx 1.8062$ , coincide with the coefficients of the identified noncausal FIR model of  $G$ .

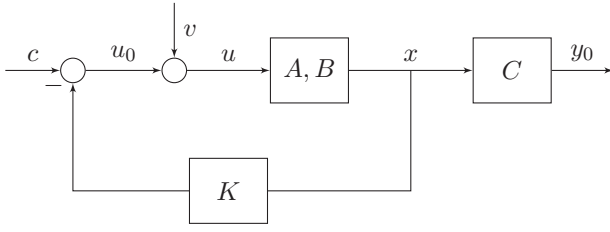


**Figure 3.** Discrete-time closed-loop control system, where  $A, B, C$  are given by (91), (92),  $x$  is the state vector,  $K$  is the LQR gain vector given by (93),  $c$  is the white, zero-mean, unit-variance command signal,  $v$  is an unknown white noise signal with a signal-to-noise ratio of 10, and  $u_0$  and  $y_0$  are the measured input and output, respectively. The plant  $G$  given by (90) is unstable, and the closed-loop system is asymptotically stable.

$$C = [0 \ 0 \ 1 \ 0 \ 0.0700 \ 0 \ -0.0144], \quad D = 0, \quad (92)$$

stabilised by an LQR controller with weighting matrices  $Q = I_7$  and  $R = 1$ , and thus the feedback gain vector is

$$K = [3.5197 \ -3.1272 \ -3.0739 \ 2.0825 \ 1.0096 \ 0.7134 \ 0.4997]. \quad (93)$$

We set  $r = d = 50$ . Let  $v$  in Figure 3 be a realisation of a zero-mean white Gaussian random process with a signal-to-noise ratio of 10. Let  $\hat{G}_{LS,\ell}$ ,  $\hat{G}_{IV,\ell}$ , and  $\hat{G}_{PEM,\ell}$  of order  $n_{\text{mod}}$  be the identified IIR models using LS, IV, and PEM, respectively, where  $\ell$  samples are used for identification. To apply IV and PEM, we use the Matlab functions `iv4(data, 'na', nmod, 'nb', nmod)` and `pem(data, nmod)`, respectively. Then we find the Laurent series of  $\hat{G}_{LS,\ell}$ ,  $\hat{G}_{IV,\ell}$ , and  $\hat{G}_{PEM,\ell}$  in the annulus that contains the unit circle and we truncate them as in (19). To do this, we express each model as the sum of an asymptotically stable part  $G_{AS}$  and a strongly unstable part  $G_{SU}$ . We then impulse  $G_{AS}(z)$  and  $G_{SU}(z^{-1})$  in order to obtain the Laurent series coefficients of  $\hat{G}_{LS,\ell}$ ,  $\hat{G}_{IV,\ell}$ , and  $\hat{G}_{PEM,\ell}$  in the annulus that contains the unit circle. Then, we compute the error in the estimated Laurent series coefficients defined by

$$\delta_\ell \triangleq \frac{1}{100} \sum_{i=1}^{100} \|\theta_{r,d} - \hat{\theta}_{r,d,\ell,i}\|_2, \quad (94)$$

where  $\hat{\theta}_{r,d,\ell,i}$  is the vector of estimated Laurent series coefficients of  $\hat{G}_{LS,\ell}$ ,  $\hat{G}_{IV,\ell}$ , or  $\hat{G}_{PEM,\ell}$  obtained from the  $i$ th experiment.

Next, we consider a noncausal FIR model with  $r = d = 50$ , and we estimate the vector of Laurent series coefficients for 100 independent experiments. We compute the error in the estimated Laurent series coefficients using (94), where  $\hat{\theta}_{r,d,\ell,i}$  in (94) is the vector of estimated

Laurent series coefficients obtained from the  $i$ th experiment using LS, IV, or PEM. Figure 4 shows  $\delta_\ell$  for LS, IV, and PEM with IIR and noncausal FIR models for  $\ell = 10,000$  samples, where the order  $n_{\text{mod}}$  of the IIR model changes between 1 and 20 and the order of the noncausal FIR model is fixed at  $r = d = 50$ . Figure 4 shows that FIR models give more accurate estimates of the Laurent series coefficients of  $G$  than IIR models for all  $1 \leq n_{\text{mod}} \leq 20$ .

In the next section, we show that the estimated Laurent series coefficients can be used to estimate the order of the system, which in turn can be used with PEM or IV to improve the accuracy of an IIR model.

## 7. Reconstructing $G$ from its noncausal FIR model

In order to reconstruct  $G$  from an approximate noncausal FIR model, we reconstruct the asymptotically stable and unstable parts of  $G$  separately using the eigen-system realisation algorithm (ERA) (Juang, 1993). Then, we obtain  $G$  by adding these two terms together as in (10). The singular values of the Hankel matrix can be used to estimate the model orders  $n_s$  of  $G_s$  and  $n_u$  of  $G_u$ . We begin with initial estimates  $\hat{n}_s \geq n_s$  and  $\hat{n}_u \geq n_u$ . For  $G_s$ , we set  $r = 2\hat{n}_s - 1$  and  $d = 0$ , and we obtain estimates of the Markov parameters of  $G_s$  using least squares, instrumental variables methods, and prediction error methods. On the other hand, for  $G_u$ , we set  $r = 0$  and  $d = 2\hat{n}_u - 1$ , and we obtain estimates of the Markov parameters of  $G_u(z^{-1})$  using least squares, instrumental variables methods, and prediction error methods. Then, we construct the Markov block–Hankel matrix

$$\mathcal{H}(H_s) \triangleq \begin{bmatrix} H_{s,1} & \cdots & H_{s,\hat{n}_s} \\ \vdots & \ddots & \vdots \\ H_{s,\hat{n}_s} & \cdots & H_{s,2\hat{n}_s-1} \end{bmatrix}, \quad (95)$$

where

$$H_s \triangleq [H_{s,0} \cdots H_{s,2\hat{n}_s-1}], \quad (96)$$

and  $\mathcal{H}(\cdot)$  is a linear mapping that constructs a Markov block–Hankel matrix from the components of the vector  $H_s$  except for  $H_{s,0}$ . The rank of  $\mathcal{H}(H_s)$  is equal to the McMillan degree of  $G_s$ . Similarly, for  $G_u(z^{-1})$ , we construct the Markov block–Hankel

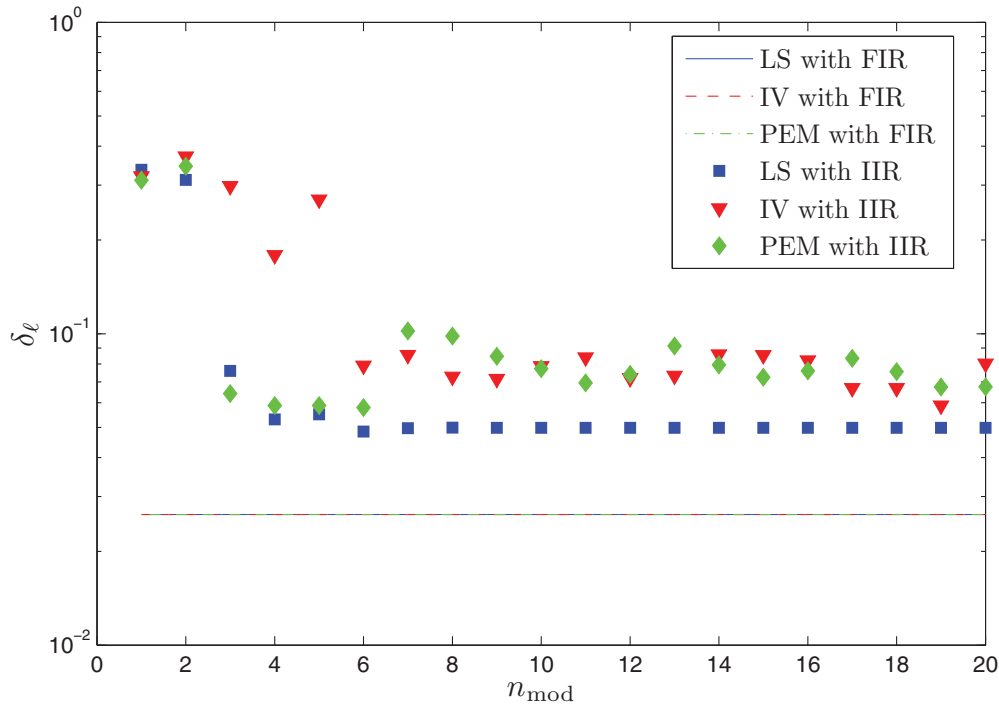


**Figure 4.**  $G(z)$  given by (90) is an unstable but not strongly unstable transfer function,  $r = d = 50$ ,  $\ell = 10,000$  samples, and  $v$  in Figure 3 is a realisation of a zero-mean white Gaussian random process with a signal-to-noise ratio of 10. The plot shows that FIR models give more accurate estimates of the Laurent series coefficients of  $G$  than IIR models for all  $1 \leq n_{\text{mod}} \leq 20$ .

matrix

$$\mathcal{H}(H_u) \triangleq \begin{bmatrix} H_{u,-1} & \cdots & H_{u,-\hat{n}_u} \\ \vdots & \ddots & \vdots \\ H_{u,-\hat{n}_u} & \cdots & H_{u,-2\hat{n}_u+1} \end{bmatrix}, \quad (97)$$

where

$$H_u \triangleq [H_{u,0} \cdots H_{u,-2\hat{n}_u+1}], \quad (98)$$

and  $\mathcal{H}(\cdot)$  constructs a Markov block–Hankel matrix from the components of the vector  $H_u$  except for  $H_{u,0}$ . The rank of  $\mathcal{H}(H_u)$  is equal to the McMillan degree of  $G_u(z^{-1})$ .

We compute the singular values of  $\mathcal{H}(H_s)$  and  $\mathcal{H}(H_u)$  and look for a large decrease in the singular values. For noise-free data, a large decrease in the singular values is evident. However, even with a small amount of noise, the large decrease in the singular values disappears, and thus the problem of estimating the model order becomes difficult (Smith, 2014).

The nuclear-norm minimisation technique given in Smith (2014) and Recht et al. (2010) provides a heuristic optimisation approach to this problem. Let  $\hat{H}_s$  be the

vector of estimated Markov parameters, where

$$\hat{H}_s \triangleq [\hat{H}_{s,0} \cdots \hat{H}_{s,2\hat{n}-1}]. \quad (99)$$

In order to estimate the order of  $G_s$ , we solve the optimisation problem

$$\underset{\tilde{H}_s(\gamma_s)}{\text{minimise}} \|\mathcal{H}(\tilde{H}_s(\gamma_s))\|_N \quad (100)$$

subject to

$$\|\tilde{H}_s(\gamma_s) - \hat{H}_s\|_F \leq \gamma_s, \quad (101)$$

where  $\gamma_s$  is varied over a range of small positive numbers. For each value of  $\gamma_s$ , we first solve the optimisation problem (100), (101), and then we construct the Markov block–Hankel matrix  $\mathcal{H}(\tilde{H}_s(\gamma_s))$  and compute its singular values. The singular values of  $\mathcal{H}(\tilde{H}_s(\gamma_s))$  that are robust to the change in  $\gamma_s$  provide an estimate of the McMillan degree of  $G_s$ . Finally, we use ERA to construct an estimate  $\hat{G}_s(z)$  of  $G_s(z)$ .

Similarly, let  $\hat{H}_u$  be the vector of estimated Markov parameters, where

$$\hat{H}_u \triangleq [\hat{H}_{u,0} \cdots \hat{H}_{u,-2\hat{n}+1}]. \quad (102)$$

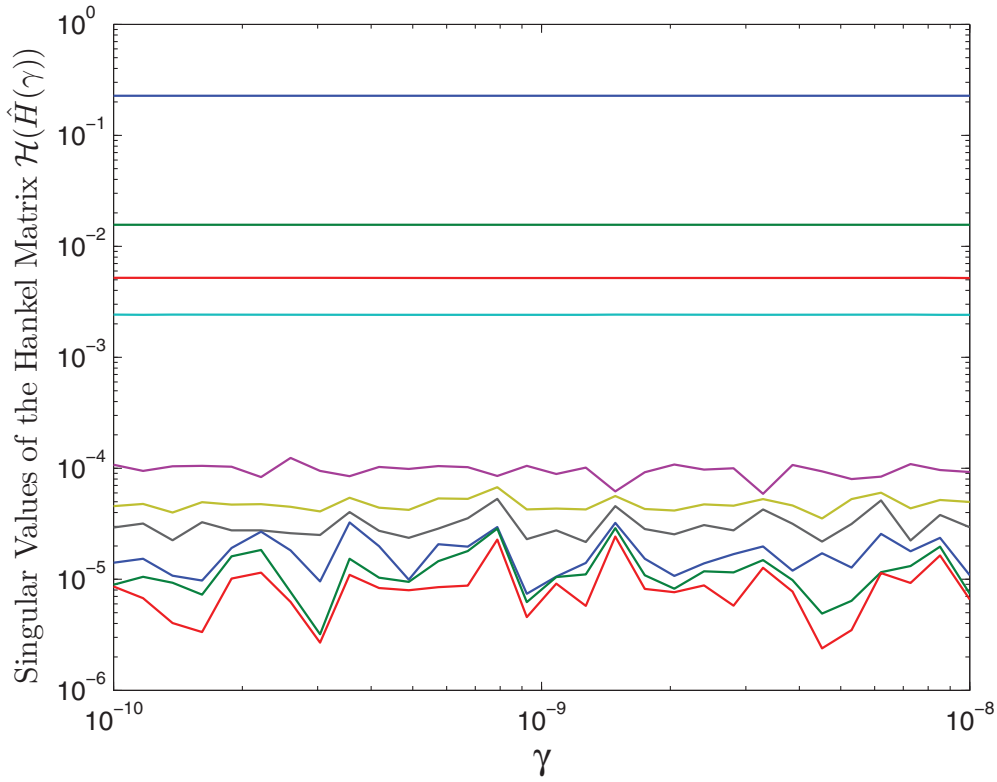


**Figure 5.** Plot of the singular values of  $\mathcal{H}(\hat{H}(\gamma_s))$  versus  $\gamma_s$ , where  $\hat{n}_s = 10$  and  $\hat{H}_s$  in (101) is the vector of estimated Markov parameters of  $G_s$  obtained using PEM with a noncausal FIR model with  $r = d = 25$ , averaged over 100 independent experiments. Note that four singular values of  $\mathcal{H}(\hat{H}(\gamma_s))$  are robust to the change in  $\gamma_s$ , which correctly yields  $\hat{n}_s = 4$  as the estimated order of  $G_s$ .

In order to estimate the order of  $G_u$ , we solve the optimisation problem

$$\underset{\hat{H}_u(\gamma_u)}{\text{minimise}} \|\mathcal{H}(\bar{H}_u(\gamma_u))\|_N \quad (103)$$

subject to

$$\|\bar{H}_u(\gamma_u) - \hat{H}_u\|_F \leq \gamma_u, \quad (104)$$

where  $\gamma_u$  is varied over a range of small positive numbers. For each value of  $\gamma_u$ , we solve the optimisation problem (103), (104), and then we construct the Markov block–Hankel matrix  $\mathcal{H}(\bar{H}_u(\gamma_u))$  and compute its singular values. The singular values of  $\mathcal{H}(\bar{H}_u(\gamma_u))$  that are robust to the change in  $\gamma_u$  provide an estimate of the McMillan degree of  $G_u$ . Finally, we use ERA to construct an estimate  $\hat{G}_u(z^{-1})$  of  $G_u(z^{-1})$ . The following example illustrates this method.

**Example 7.1:** Consider the system (90). We choose  $c$  in Figure 3 to be a realisation of a stationary white random process  $\mathcal{C}$  with Gaussian probability density function  $\mathcal{N}(0, 1)$ . Let  $v$  be a white noise signal with a signal-to-noise ratio of 20. We set  $r = d = 25$ , and  $\ell = 10,000$  points

and identify a noncausal FIR model of  $G$ . The estimated Markov parameters are averaged over 100 experiments.

To choose the model order for  $G_s(z)$ , we set  $\hat{n}_s = 10$  and solve the optimisation problem (100), (101) for values of  $\gamma_s$  ranging from  $10^{-10}$  to  $10^{-8}$ . For each value of  $\gamma_s$ , we first find the optimal  $\hat{H}_s(\gamma_s)$ , and then we construct the Markov block–Hankel matrix  $\mathcal{H}(\hat{H}_s(\gamma_s))$  and compute its singular values. Figure 5 shows the singular values of the Hankel matrix  $\mathcal{H}(\hat{H}_s(\gamma_s))$  versus  $\gamma_s$ . Figure 5 shows that four singular values of  $\mathcal{H}(\hat{H}_s(\gamma_s))$  are robust to the change in  $\gamma_s$ , which correctly yields  $\hat{n}_s = 4$  as the estimated order of  $G_s$ . Using ERA, we obtain

$$\hat{G}_s(z) = \frac{0.0732z^3 + 0.0211z^2 - 0.0039z + 0.0112}{z^4 + 1.275z^3 + 0.4491z^2 + 0.2447z + 0.1721}. \quad (105)$$

Similarly, for  $G_u(z^{-1})$ , we set  $\hat{n}_u = 10$  and solve the optimisation problem (103), (104) for values of  $\gamma_u$  ranging from  $10^{-10}$  to  $10^{-8}$ . For each value of  $\gamma_u$ , we first find the optimal  $\hat{H}_u(\gamma_u)$ , and then we construct the Markov block–Hankel matrix  $\mathcal{H}(\hat{H}_u(\gamma_u))$  and compute its singular values. Figure 6 shows the singular values of the Hankel matrix  $\mathcal{H}(\hat{H}_u(\gamma_u))$  versus  $\gamma_u$ . Figure 6 shows

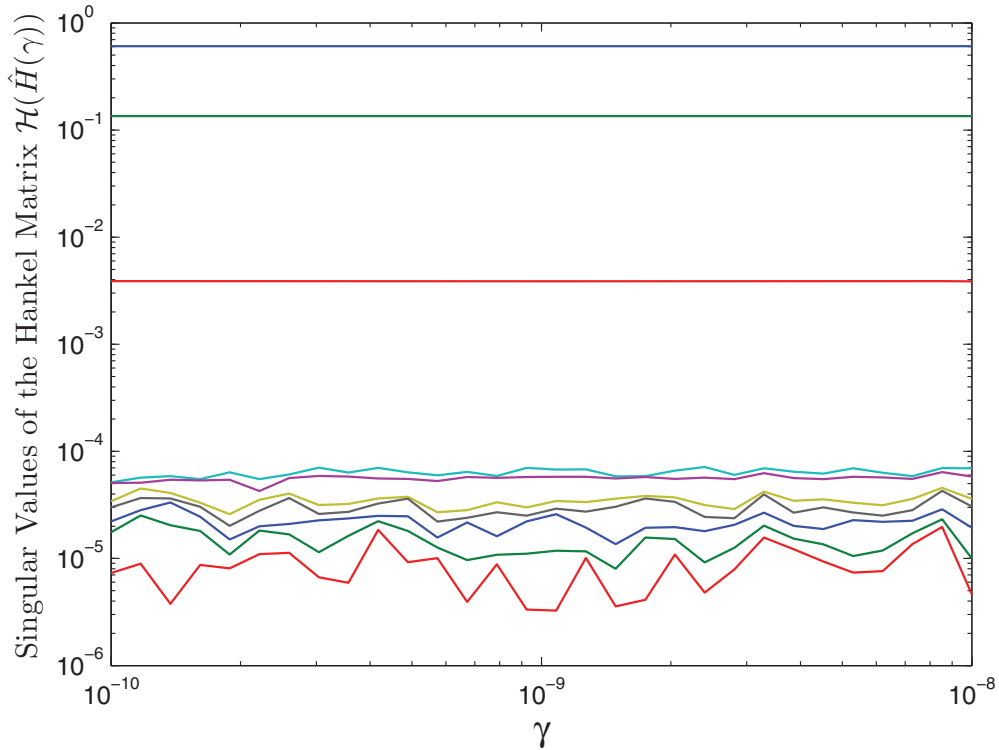


**Figure 6.** Plot of the singular values of  $\mathcal{H}(\hat{H}(\gamma_u))$  versus  $\gamma_u$ , where  $\hat{n}_u = 10$  and  $\hat{H}_u$  in (104) is the vector of estimated Markov parameters of  $G_u(z^{-1})$  obtained using PEM with a noncausal FIR model with  $r = d = 25$ , averaged over 100 independent experiments. Note that three singular values of  $\mathcal{H}(\hat{H}(\gamma_u))$  are robust to the change in  $\gamma_u$ , which correctly yields  $\hat{n}_u = 3$  as the estimated order of  $G_u$ .

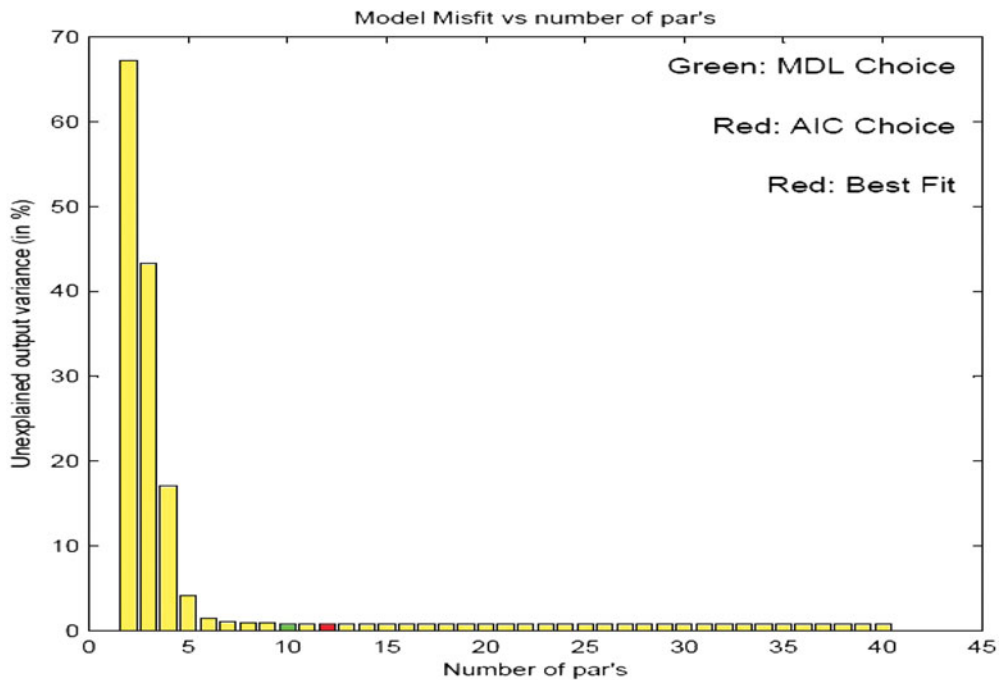


**Figure 7.** The Matlab System Identification Toolbox is used to obtain the number of parameters of the ARX model that gives the best fit of  $G$ , which has 12 parameters as indicated by this figure. Moreover, the orders of the denominator, numerator, and input-output delay of the ARX model are  $n_a = 9$ ,  $n_b = 3$ ,  $n_k = 1$ , respectively..

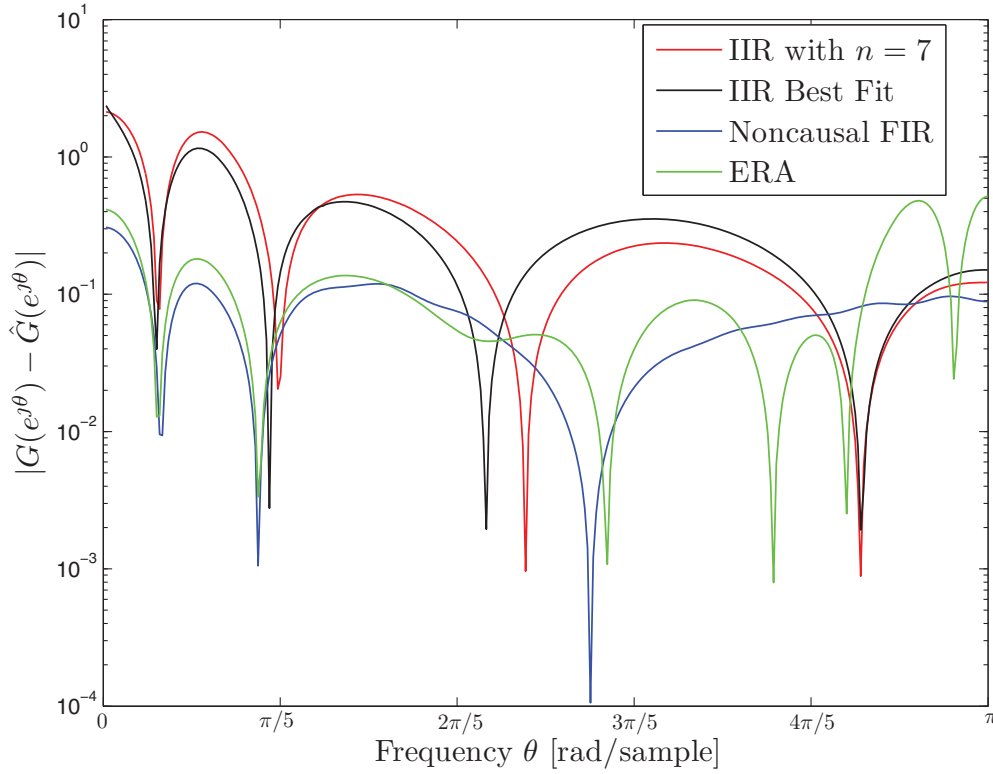


**Figure 8.** Bode plots of  $G - \hat{G}_{\text{IIR}}$ ,  $G - \hat{G}_{\text{IIR, BestFit}}$ ,  $G - \hat{G}_{\text{FIR}}$ , and  $G - \hat{G}_{\text{ERA}}$ . Note that the noncausal FIR estimate  $\hat{G}_{r,d}$  yields the smallest error in the estimated frequency response of  $G$ .

that three singular values of  $\mathcal{H}(\bar{H}_u(\gamma_u))$  are robust to the change in  $\gamma_u$ , which correctly yields  $\hat{n}_u = 3$  as the estimated order of  $G_u$ . Using ERA, we obtain

$$\hat{G}_u(z^{-1}) = \frac{0.0093z^3 - 0.0883z^2 + 0.0088z - 0.0006}{z^3 - 1.700z^2 + 0.9321z - 0.1550}, \quad (106)$$

that is,

$$\hat{G}_u(z) = \frac{0.0006z^3 - 0.0088z^2 + 0.0883z - 0.0093}{0.1550z^3 - 0.9321z^2 + 1.7z - 1}. \quad (107)$$

It follows that the estimate  $\hat{G}$  of  $G$  is

$$\begin{aligned} \hat{G}_{\text{ERA}}(z) &= \hat{G}_s(z) + \hat{G}_u(z) \\ &= \frac{0.0006z^7 + 0.0033z^6 + 0.0123z^5 + 0.2036z^4 - 0.0062z^3 - 0.0223z^2 + 0.0358z - 0.0128}{0.155z^7 - 0.7344z^6 + 0.5805z^5 + 0.7870z^4 - 0.7135z^3 - 0.1936z^2 + 0.0478z - 0.1721}. \end{aligned} \quad (108)$$

The Matlab system identification toolbox is used to obtain the number of parameters of the ARX model that

gives the best fit of  $G$ , which has 12 parameters as indicated by the solid red rectangle in Figure 7. Moreover, the orders of the denominator, numerator, and input–output delay for this ARX model are  $n_a = 9$ ,  $n_b = 3$ ,  $n_k = 1$ , respectively, as suggested by the Matlab system identification toolbox.

Figure 8 shows the difference between the Bode plots of  $G$  and the estimates  $\hat{G}_{\text{IIR}}$  obtained using PEM with an IIR model with order  $n_{\text{mod}} = 7$ ,  $\hat{G}_{\text{IIR, BestFit}}$  obtained using PEM with an ARX model with orders  $n_a = 9$ ,  $n_b = 3$ ,  $n_k = 1$ ,  $\hat{G}_{\text{ERA}}$  in (108), and  $\hat{G}_{r,d}$  obtained using PEM with a noncausal FIR model with  $r = d = 25$ . Note that the noncausal FIR estimate,  $\hat{G}_{r,d}$ , yields the smallest error in the estimated frequency response of  $G$ . Moreover, note that  $G_{\text{ERA}}$  gives better estimates than  $\hat{G}_{\text{IIR}}$  and  $\hat{G}_{\text{IIR, BestFit}}$ .

## 8. Conclusions and future research

In this paper, we used noncausal FIR models for closed-loop identification of open-loop-unstable plants. To identify the noncausal model, we delayed the measured output relative to the measured input. We found that the identified FIR model approximates the Laurent series of the plant inside the annulus of analyticity lying between the disk of stable poles and the punctured plane of unstable

poles. We presented examples to compare the accuracy of the identified model obtained using least squares, instrumental variables methods, and prediction error methods for both IIR and noncausal FIR models under arbitrary noise that is fed back into the loop. Numerical examples showed that using noncausal FIR models for identification of unstable systems in closed loop can give better estimates than using IIR models. We used nuclear norm minimisation to estimate the orders of the asymptotically stable and unstable parts of the plant, which can improve the identification accuracy for IIR systems. Finally, we reconstructed an IIR model of the system from its asymptotically stable and unstable parts using the eigensystem realisation algorithm.

Future research will focus on three extensions. First, the results in this paper assume that the plant has no poles on the unit circle. A potential approach to this problem is to scale the coefficients of the Laurent series of the plant in the annulus that contains the unit circle as in (22) so that the effective plant has no poles with unit modulus. Next, the command signal and the input noise signal in this paper were assumed to be white. The case where the command signal is arbitrary or the input noise signal is coloured can arise in practice and remains to be addressed. Finally, to enhance persistency, an external noise signal, which is either known or unknown, can be added to the control signal at the expense of performance degradation. However, in some cases, the improved identification speed and accuracy may warrant this degradation, and this tradeoff remains to be explored.

## Acknowledgments

The authors would like to thank Shicong Dai for help in proving Lemma 4.1. This research was partially supported by NASA grant NNX14AJ55A.

## Disclosure statement

No potential conflict of interest was reported by the authors.

## References

- Aljanaideh, K., Coffer, B.J., & Bernstein, D.S. (2013). *Closed-loop identification of unstable systems using noncausal FIR models*. Proceedings of American Control conference (pp. 1669–1674), Washington, DC.
- Cerone, V., Piga, D., & Regruto, D. (2013). Fixed-order FIR approximation of linear systems from quantized input and output data. *Systems & Control Letters*, 62, 1136–1142.
- Chai, L., Zhang, J., Zhang, C., & Mosca, E. (2005). *From IIR to FIR digital MIMO models: A constructive Hankel norm approximation method*. Proceedings of IEEE conference on Decision and Control and European Control conference (pp. 5893–5898). IEEE.
- Forsell, U., & Ljung, L. (1999). Closed-loop identification revisited. *Automatica*, 35, 1215–1241.
- Forsell, U., & Ljung, L. (2000a). A projection method for closed-loop identification. *IEEE Transactions on Automatic Control*, 45, 2101–2106.
- Forsell, U., & Ljung, L. (2000b). Identification of unstable systems using output-error and Box–Jenkins model structures. *IEEE Transactions on Automatic Control*, 45, 137–141.
- Gamelin, T.W. (2001). *Complex analysis*. New York, NY: Springer.
- Gilson, M., & Van den Hof, P. (2005). Instrumental variable methods for closed-loop system identification. *Automatica*, 41, 241–249.
- Gross, E., Tomizuka, M., & Messner, W. (1994). Cancellation of discrete time unstable zeros by feedforward control. *Journal of Dynamic Systems, Measurement, and Control*, 116, 33–38.
- Gustavsson, I., Ljung, L., & Söderström, T. (1977). Identification of processes in closed loop—identifiability and accuracy aspects. *Automatica*, 13, 59–75.
- Hjalmarsson, H., & Forsell, U. (1999). *Maximum likelihood estimation of models with unstable dynamics and non-minimum phase noise zeros*. Proceedings of 14th IFAC World Congress (pp. 13–18), Beijing, China.
- Hjalmarsson, H., Gevers, M., & de Bruyne, F. (1996). For model-based control design, closed-loop identification gives better performance. *Automatica*, 32, 1659–1673.
- Hjalmarsson, H., Welsh, J.S., & Rojas, C.R. (2012, July). *Identification of Box–Jenkins models using structured ARX models and nuclear norm relaxation*. Proceedings of SYSID (pp. 322–327), Brussels, Belgium.
- Ho, B., & Kalman, R. (1966). Efficient construction of linear state variable models from input/output functions. *Regelungstechnik*, 14, 545–548.
- Hunt, L., Meyer, G., & Su, R. (1996). Noncausal inverses for linear systems. *IEEE Transactions on Automatic Control*, 41, 608–611.
- Juang, J.N. (1993). *Applied system identification*. Upper Saddle River, NJ: Prentice-Hall.
- Landau, I. (2001). Identification in closed-loop: A powerful design tool (better design models, simple controllers). *Control Engineering Practice*, 9, 51–65.
- Ljung, L. (1999). *System identification: Theory for the user* (2nd ed.). Upper Saddle River, NJ: Prentice-Hall Information and Systems Sciences.
- Ljung, L. (2002). Prediction error estimation methods. *Circuits, Systems and Signal Processing*, 21, 11–21.
- Ljung, L., & McKelvey, T. (1996). Subspace identification from closed-loop data. *Signal Processing*, 52, 209–215.
- Markovskiy, I. (2012, July). *How effective is the nuclear norm heuristic in solving data approximation problems?* Proceedings of SYSID (pp. 316–321), Brussels, Belgium.
- Recht, B., Fazel, M., & Parrilo, P.A. (2010). Guaranteed minimum-rank solutions of linear matrix equations via nuclear norm minimization. *SIAM Review*, 52, 471–501.
- Rigney, B.P., Pao, L.Y., & Lawrence, D.A. (2009). Nonminimum phase dynamic inversion for settle time applications. *IEEE Transactions on Control Systems Technology*, 17, 989–1005.
- Smith, R.S. (2014). Frequency domain subspace identification using nuclear norm minimization and Hankel matrix

- realizations. *IEEE Transactions on Automatic Control*, 59, 2886–2896.
- Söderström, T., & Stoica, P. (1981). Comparison of some instrumental variable methods-consistency and accuracy aspects. *Automatica*, 17, 101–115.
- Söderström, T., & Stoica, P. (1983). *Instrumental variable methods for system identification*. Berlin: Springer-Verlag.
- Söderström, T., & Stoica, P. (2002). Instrumental variable methods for system identification. *Circuits, Systems and Signal Processing*, 21, 1–9.
- Stoica, P., Söderström, T., & Friedlander, B. (1985). Optimal instrumental variable estimates of the AR parameters of an ARMA process. *IEEE Transactions on Automatic Control*, 30, 1066–1074.
- Tomizuka, M. (1987). Zero phase error tracking algorithm for digital control. *Journal of Dynamic Systems, Measurement, and Control*, 109, 65–68.
- Usevich, K., & Markovsky, I. (2012, July). Structured low-rank approximation as a rational function minimization. *Proceedings of SYSID* (pp. 722–727), Brussels, Belgium.
- Verhaegen, M. (1993). Application of a subspace model identification technique to identify LTI systems operating in closed-loop. *Automatica*, 29, 1027–1040.
- Widrow, B., & Walach, E. (1996). *Adaptive inverse control*. Upper Saddle River, NJ: Prentice Hall.
- Yamamoto, Y., Anderson, B.D., Nagahara, M., & Koyanagi, Y. (2003). Optimizing FIR approximation for discrete-time IIR filters. *IEEE Signal Processing Letters*, 10, 273–276.